iScience

CellPress

Article

Cytosolic Ca^{2+} Modulates Golgi Structure Through PKCα-Mediated GRASP55 Phosphorylation

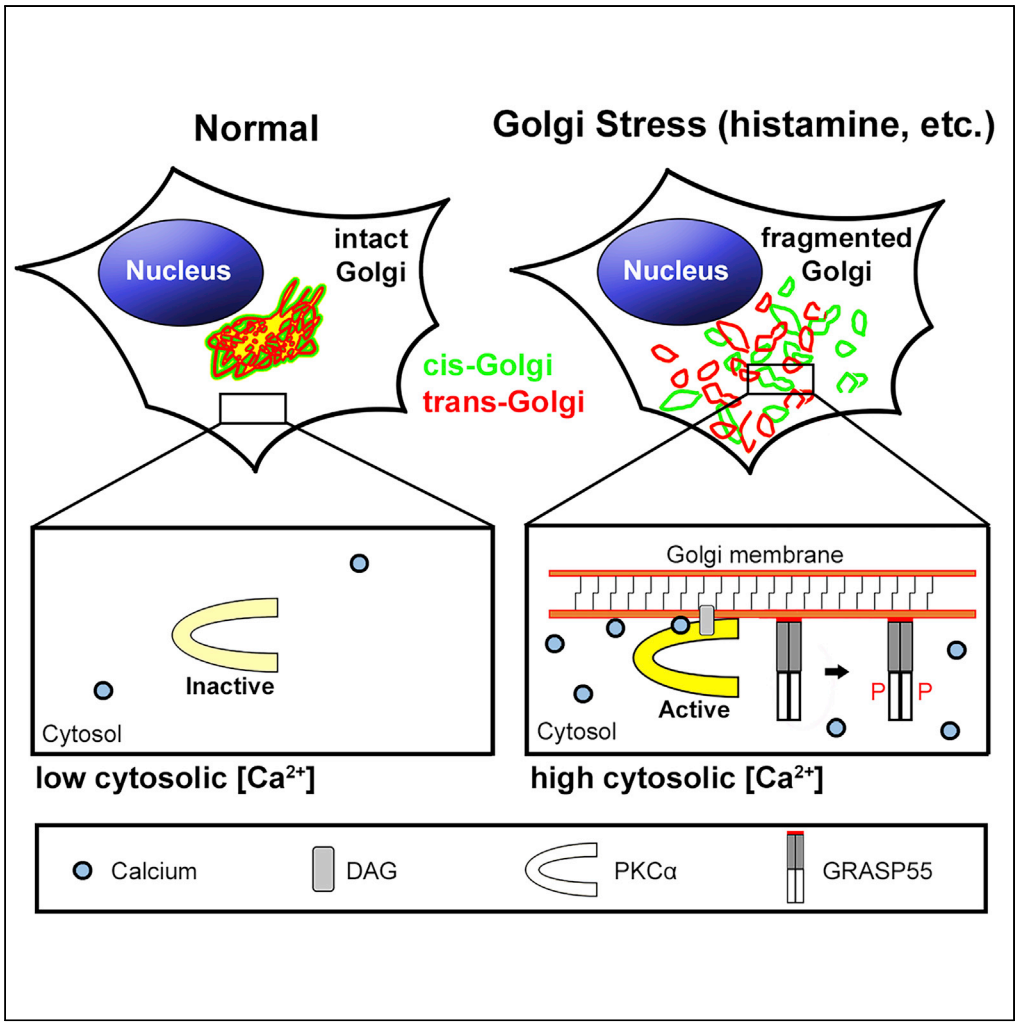

Stephen Ireland, Saiprasad Ramnarayanan, Mingzhou Fu, ..., Jie Li, Dabel Emebo, Yanzhuang Wang

yzwang@umich.edu

HIGHLIGHTS

Thapsigargin (TG) treatment leads to Golgi fragmentation independent of ER stress

TG induces Golgi fragmentation through elevated cytosolic Ca^{2+}

TG-induced cytosolic Ca^{2+} spikes activate PKCα that phosphorylates GRASP55

Histamine modulates the Golgi structure and function by a similar mechanism

Ireland et al., iScience *23*, 100952
March 27, 2020
https://doi.org/10.1016/j.isci.2020.100952

iScience

CellPress

Article

Cytosolic Ca^{2+} Modulates Golgi Structure Through PKCα-Mediated GRASP55 Phosphorylation

Stephen Ireland,[1] Saiprasad Ramnarayanan,[1] Mingzhou Fu,[1] Xiaoyan Zhang,[1] Jianchao Zhang,[1] Jie Li,[1] Dabel Emebo,[1] and Yanzhuang Wang[1,2,3,*]

SUMMARY

It has been well documented that the ER responds to cellular stresses through the unfolded protein response (UPR), but it is unknown how the Golgi responds to similar stresses. In this study, we treated HeLa cells with ER stress inducers, thapsigargin (TG), tunicamycin (Tm), and dithiothreitol (DTT), and found that only TG treatment resulted in Golgi fragmentation. TG induced Golgi fragmentation at a low dose and short time when UPR was undetectable, indicating that Golgi fragmentation occurs independently of ER stress. Further experiments demonstrated that TG induces Golgi fragmentation through elevating intracellular Ca^{2+} and protein kinase Cα (PKCα) activity, which phosphorylates the Golgi stacking protein GRASP55. Significantly, activation of PKCα with other activating or inflammatory agents, including phorbol 12-myristate 13-acetate and histamine, modulates Golgi structure in a similar fashion. Hence, our study revealed a novel mechanism through which increased cytosolic Ca^{2+} modulates Golgi structure and function.

INTRODUCTION

In mammalian cells, the Golgi apparatus is characterized by a multilayer stacked structure of ~5–7 flattened cisternal membranes, and stacks are often laterally linked to form a ribbon located in the perinuclear region of the cell (Tang and Wang, 2013; Wang and Seemann, 2011). The exact mechanism of Golgi stack formation is not fully understood, but it has been shown that the Golgi re-assembly stacking protein of 55 kDa (GRASP55, also called GORASP2) and its homolog GRASP65 (GORASP1) play essential roles in Golgi stacking (Wang et al., 2003; Zhang and Wang, 2015). Both GRASPs are peripheral membrane proteins that share similar domain structures and overlapping functions (Wang and Seemann, 2011). GRASP65 is predominantly concentrated in the cis Golgi, whereas GRASP55 is localized on *medial-trans* cisternae. Both GRASPs form *trans*-oligomers through their N-terminal GRASP domains that "glue" adjacent Golgi cisternae together into stacks (Wang et al., 2003; Xiang and Wang, 2010) and ribbons (Feinstein and Linstedt, 2008; Puthenveedu et al., 2006). GRASP oligomerization is regulated by phosphorylation; mitotic phosphorylation of GRASP55 and GRASP65 at the C-terminal serine/proline-rich (SPR) domain inhibits oligomerization and results in Golgi cisternal unstacking and disassembly (Tang et al., 2012; Wang et al., 2005; Xiang and Wang, 2010).

The Golgi exhibits different morphology in different cell types and tissues as well as under different conditions. For example, in many secretory cells such as Brunner's gland of platypus, the Golgi forms large, well-formed stacks (Krause, 2000), whereas electron micrographs show reorganization of Golgi membranes in prolactin cells of female rats upon cessation of a sucking stimulus (Rambourg et al., 1993). In neurons, increased neuronal activity causes dispersal of the Golgi at the resolution of light microscopy (Thayer et al., 2013). In Alzheimer disease, the Golgi membranes are dispersed and fragmented in neurons from human brain and mouse models (Joshi et al., 2015). Golgi fragmentation is also observed in other neurodegenerative diseases, including Parkinson (Mizuno et al., 2001) and Huntington (Hilditch-Maguire et al., 2000) diseases and amyotrophic lateral sclerosis (ALS) (Fujita and Okamoto, 2005; Gonatas et al., 1998; Mourelatos et al., 1996). In addition, the Golgi has also been shown to be fragmented in lung, prostate, and breast cancers (Petrosyan et al., 2014; Sewell et al., 2006; Tan et al., 2016). A plausible hypothesis is that the Golgi adjusts its structure and function in response to different physiological and pathological conditions; however, the molecular mechanisms that control Golgi structure and function under disease conditions are so far not well understood.

[1]Department of Molecular, Cellular and Developmental Biology, University of Michigan, Biological Sciences Building, 1105 North University Avenue, Ann Arbor, MI 48109-1085, USA

[2]Department of Neurology, University of Michigan School of Medicine, Ann Arbor, MI 48109-1085, USA

[3]Lead Contact

*Correspondence: yzwang@umich.edu

https://doi.org/10.1016/j.isci.2020.100952

The Golgi structure can be modulated experimentally such as by molecular manipulations of GRASP55 and GRASP65. Microinjection of antibodies against GRASP55 or GRASP65 into cells inhibits post-mitotic stacking of newly formed Golgi cisternae (Wang et al., 2003, 2008). Knockdown (KD, by siRNA) or knockout (KO, by CRISPR/Cas9) of either GRASP reduces the number of cisternae per stack (Sutterlin et al., 2005; Tang et al., 2010), whereas simultaneous depletion of both GRASPs causes fragmentation of the entire Golgi stack (Bekier et al., 2017; Xiang and Wang, 2010). Expression of non-phosphorylatable GRASP65 mutants enhances Golgi stacking in interphase and inhibits Golgi disassembly in mitosis (Tang et al., 2010). Because GRASPs play critical roles in Golgi structure formation, it is reasonable to speculate that physiological and pathological cues may trigger Golgi fragmentation through GRASP55/65 modification, such as phosphorylation (Ahat et al., 2019a; Li et al., 2019a). Using GRASPs as tools to manipulate Golgi stack formation, it has been demonstrated that Golgi cisternal unstacking accelerates protein trafficking but impairs accurate glycosylation and sorting (Bekier et al., 2017; Xiang et al., 2013). In addition, GRASP depletion also affects other cellular activities such as cell attachment, migration, growth, and autophagy (Ahat et al., 2019b; Zhang et al., 2018, 2019).

Protein kinase C (PKC) is a large family of multifunctional serine/threonine kinases that are activated by signals such as increases in the concentration of diacylglycerol (DAG) and/or intracellular calcium ions (Ca^{2+}). In cells, PKCs are mainly cytosolic, but transiently localize to membranes such as endosomes and Golgi upon activation (Chen et al., 2004; El Homasany et al., 2005). Membrane association of PKC is via a C1 domain that interacts with DAG in the membrane. Conventional PKCs (cPKCs) also contain a C2 domain that binds Ca^{2+} ions, which further enhances their membrane association and activity (Nishizuka, 1995). Knockdown of atypical PKCs (aPKCs) using siRNA causes a reduction in peripheral ERGIC-53 clusters without affecting the Golgi morphology (Farhan et al., 2010). In addition, increased PKC activity has been implicated in cancer (Cooke et al., 2017; Kim et al., 2013), but the mechanism by which PKC may contribute to invasion, inflammation, tumorigenesis, and metastasis is not fully understood (Griner and Kazanietz, 2007).

In this study, we performed high-resolution microscopy and biochemistry experiments to determine how the Golgi responds to cellular stresses such as ER stress. Although not all ER stress inducers caused Golgi fragmentation, treatment of cells with the Ca^{2+}-ATPase inhibitor thapsigargin (TG) resulted in Golgi fragmentation with a low dose and short time in which ER stress was undetectable, indicating that Golgi fragmentation occurs independently of ER stress. Further experiments demonstrated that TG-induced cytosolic Ca^{2+} spikes activate PKC that phosphorylates GRASP55. Interestingly, inflammatory factors such as histamine modulate the Golgi structure through a similar mechanism. Thus, we have uncovered a novel pathway through which cytosolic Ca^{2+} modulates the Golgi structure and function.

RESULTS

TG Induces Golgi Fragmentation and UPR

It has been hypothesized that ER stress and the unfolded protein response (UPR) cause Golgi fragmentation and dysfunction through overloading misfolded proteins into the Golgi (Oku et al., 2011). To test this hypothesis, we performed a time course treatment of HeLa cells with a well-known UPR inducer, TG, which specifically blocks the sarcoendoplasmic reticulum Ca^{2+} transport ATPase (SERCA) (Xu et al., 2004) and causes Ca^{2+} dysregulation (Ito et al., 2015). We assessed the Golgi morphology by co-staining the cells for GM130, a cis-Golgi marker, and TGN46, a protein in the *trans*-Golgi network. As shown in Figures 1A and 1B, the Golgi became fragmented after TG treatment, and the response was linear over time (Figures 1A, 1B, and S1A). Although Golgi fragmentation was more obvious after a longer treatment, it became detectable in shorter treatments such as 10 min. More careful examination of the Golgi morphology by super-resolution fluorescence microscopy demonstrated that the Golgi ribbon was broken down, as the Golgi appeared as disconnected puncta. The stacks were also defective, as indicated by the separation of GM130 and TGN46 signals (Figures 1C and 1D).

To correlate Golgi fragmentation with UPR, we performed Western blot of TG-treated cells to assess the levels of several UPR markers, including phosphorylated eukaryotic translation initiation factor 2A eIF2α (p-eIF2α), the ER chaperone binding of immunoglobulin protein (Bip), and the CCAAT-enhancer-binding protein homologous protein (CHOP). As shown in Figures 1E–1G, longer term TG treatment, for example, 2 h or longer, caused UPR, as indicated by the increase of all three markers. When the treatment was reduced to 30 min, only the p-eIF2α level increased, whereas Bip and CHOP did not change. This indicates

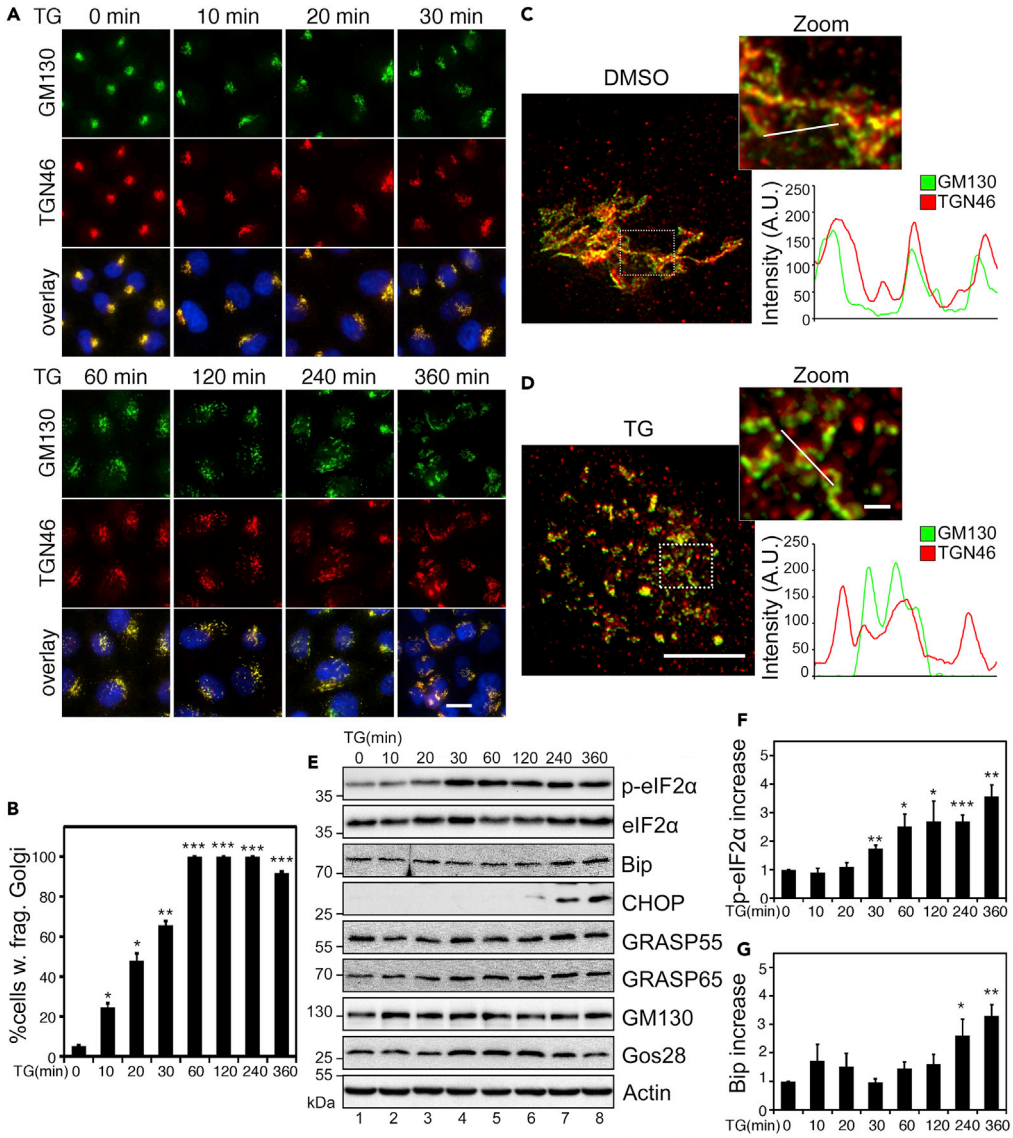

Figure 1. TG Induces Golgi Fragmentation and UPR

(A) Short-term TG treatment causes Golgi fragmentation. HeLa cells were treated with 250 nM TG, fixed at the indicated time points, and stained for GM130 (cis-Golgi) and TGN46 (*trans*-Golgi). Scale bar, 20 μm.

(B) Quantitation of (A) for cells with fragmented Golgi using GM130 as the Golgi marker.

(C and D) Super-resolution images of DMSO- (C) and TG-treated (D) HeLa cells. Cells were treated with 2 μM TG for 1 h, stained as in (A), and imaged with a Leica SP8 STED microscope. Indicated areas are enlarged and shown on the right as merged GM130 (green) and TGN46 (red). To quantify Golgi unstacking in these images, relative fluorescence intensity was plotted along a random line through the Golgi region. Note the agreement in peaks in control (C) and relative disagreement in peaks in the TG-treated cell (D). Scale bar in main images, 5 μm; in inserts, 1 μm.

(E) Longer term TG treatment results in ER stress. Cells treated as in (A) were analyzed by Western blot of indicated proteins. Note that TG treatment increases the levels of p-eIF2α, Bip, and CHOP.

(F–G) Quantitation of the ratio of p-eIF2α/eIF2α and the Bip levels from (E), with the no-treatment control normalized to 1. All quantitation results are shown as mean ± SEM from at least three independent experiments; statistical analyses were performed using two-tailed Student's *t*-tests (*$p \leq 0.05$; **$p \leq 0.01$; ***$p \leq 0.001$).

that the minimal time for UPR to occur is ~30 min under our experimental conditions. Consistently, no significant increase in the level of any of these UPR markers was detected when the treatment was reduced to below 30 min. Interestingly, the Golgi in a significant proportion of cells was fragmented at this time. Golgi fragmentation was obvious with 10-min TG treatment when UPR was undetectable and became more

prevalent at 30-min treatment (Figures 1A and 1B). The fact that Golgi fragmentation occurs earlier than UPR indicates that Golgi fragmentation is unlikely a downstream effect of ER stress, but rather occurs independently of UPR.

It is worth mentioning that TG treatment did not affect the level of key Golgi structural proteins, including the Golgi stacking proteins GRASP55 and GRASP65, the Golgi tethering protein GM130, and the Golgi SNARE Gos28 (Figure 1E), indicating that TG induces Golgi fragmentation likely through modification rather than degradation of Golgi structural proteins. In addition, TG-induced Golgi fragmentation is reversible; when TG was washed out, the Golgi structure gradually returned to its normal shape (Figures S1B–S1D). Consistently, TG-treatment did not induce apoptosis as shown by Annexin V staining. In contrast, staurosporine treatment, which is known to induce apoptosis, increased Annexin V cell surface staining (Figures S1D and S1E). In addition, TG treatment did not seem to affect the organization of the actin and microtubule cytoskeleton (Figures S1F and S1G).

Tunicamycin or Dithiothreitol Treatment Induces UPR but Not Golgi Fragmentation

To test whether the hypothesis that Golgi fragmentation occurs independently of UPR applies only to TG treatment or also to other ER stress inducers, we repeated the same set of experiments by treating cells with tunicamycin (Tm), an antibiotic that induces ER stress by inhibiting N-glycosylation and the accumulation of misfolded proteins in the ER lumen. Tm treatment did not affect the Golgi morphology after 360 min, as indicated by the GM130 and TGN46 signals (Figures S2A–S2C). Further analysis of Tm-treated cells by electron microscopy (EM) also did not reveal any significant changes in the Golgi structure (Figure S2D). The treatment indeed induced UPR, as indicated by the robust increase in the p-eIF2α, Bip, and CHOP levels, in particular after 120 min (Figures S2E–S2G). Six-hour Tm treatment increased the width of the ER cisternae and caused ER fragmentation (Figure S2H). As Tm, dithiothreitol (DTT) treatment also did not cause Golgi fragmentation, although Bip and CHOP levels increased significantly after 120 min of treatment (Figures S3A–S3D). We also performed super-resolution microscopy to examine the Golgi structure in parallel after Tm, DTT, or TG treatment. Similar to that observed in control cells, the Golgi structure is intact in Tm- and DTT-treated cells, with extensive overlap between *cis*- and *trans*-Golgi markers, whereas TG treatment caused not only fragmentation of the Golgi structure but also separation of *cis*- and *trans*-Golgi markers (Figures S3E and S3F). Taken together, these results indicate that ER stress is unlikely a direct cause of Golgi fragmentation.

TG Induces Golgi Fragmentation Prior to UPR Through Elevated Cytosolic Ca^{2+}

We next sought to decouple the Golgi stress response from UPR after TG treatment. As a complementary approach to the timecourse experiment shown in Figure 1, we titrated TG (1–250 nM) in the treatment. Here we treated cells for 20 min, a time point prior to UPR becoming detectable when cells were treated with 250 nM TG (Figure 1). The results showed that Golgi fragmentation increased linearly in response to the increasing TG concentration, and importantly, TG at low doses (1–250 nM) effectively caused Golgi fragmentation (Figures 2A and 2B). For comparison, we also assessed UPR in the same cells. As shown in Figures 2C–2E, treatment of cells with up to 250 nM TG for 20 min did not cause UPR as indicated by the p-eIF2α and Bip levels. These results indicate that TG triggers Golgi fragmentation independent of ER stress. Furthermore, we carried out similar experiments in normal rat kidney (NRK) cells and RAW 264.7 murine macrophages and obtained similar results (Figure S4), indicating that the effect of TG treatment on the Golgi structure is not cell-type specific.

We next asked how TG treatment induces Golgi fragmentation. Knowing that TG increases cytosolic Ca^{2+} (Jones and Sharpe, 1994), we employed the membrane permeable Ca^{2+} chelator BAPTA-AM to test whether TG induces Golgi fragmentation through cytosolic Ca^{2+}. We pre-treated cells with BAPTA-AM alone (60 μM) for 30 min and then with or without TG (100 nM) for 0, 15, 30, and 60 min (Figures 2F and 2G). The result showed that BAPTA-AM significantly prevented TG-induced Golgi fragmentation, whereas BAPTA-AM alone did not affect the Golgi morphology. Subsequent EM analysis confirmed TG-induced Golgi fragmentation and its rescue by BAPTA-AM (Figures 2H and 2I). TG treatment reduced the number of cisternae per stack and the length of cisternae but increased the number of vesicles surrounding each stack. These effects were largely abolished by the addition of BAPTA-AM. These results demonstrated that cytosolic Ca^{2+} is required for TG-induced Golgi fragmentation. Consistent with this notion, treatment of cells with a Ca^{2+} ionophore, ionomycin (Io), also caused Golgi fragmentation (Figures S5A and S5B). Therefore, the driving force behind TG-induced Golgi fragmentation is the elevated cytosolic Ca^{2+}.

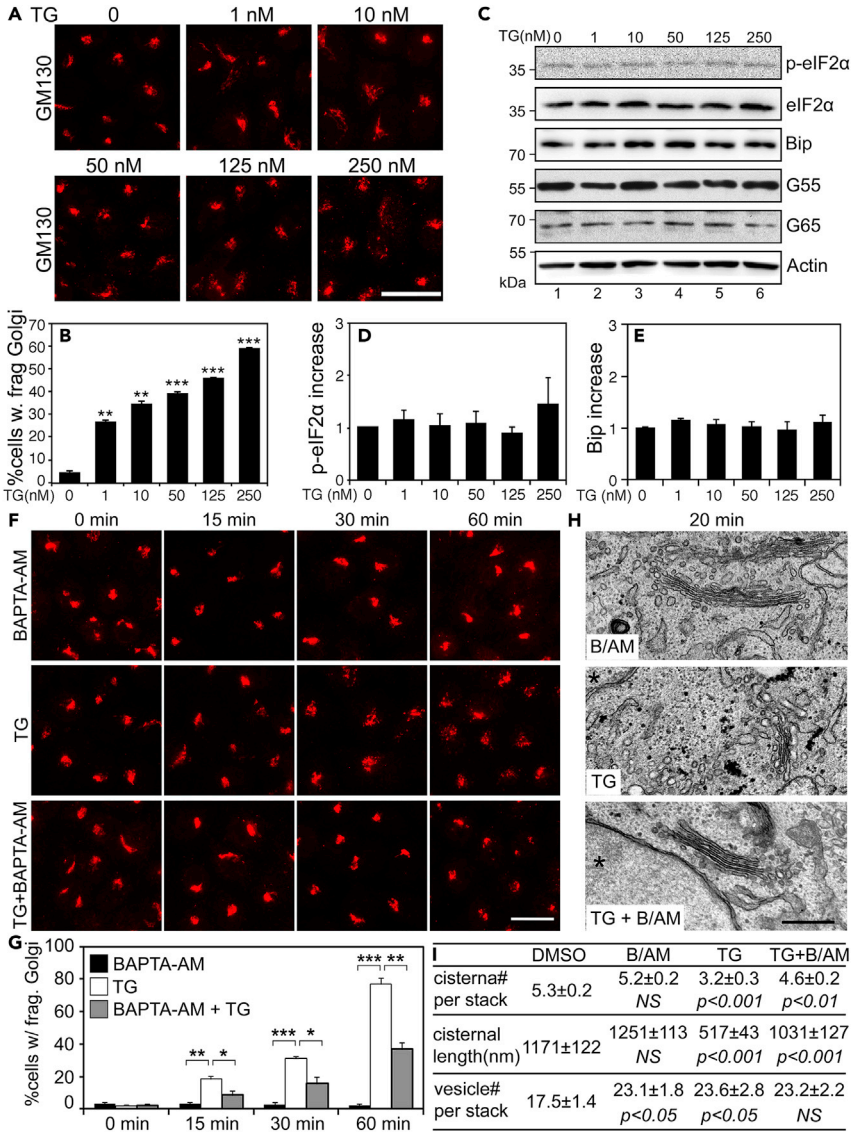

I	DMSO	B/AM	TG	TG+B/AM
cisterna# per stack	5.3±0.2	5.2±0.2 *NS*	3.2±0.3 *p<0.001*	4.6±0.2 *p<0.01*
cisternal length(nm)	1171±122	1251±113 *NS*	517±43 *p<0.001*	1031±127 *p<0.001*
vesicle# per stack	17.5±1.4	23.1±1.8 *p<0.05*	23.6±2.8 *p<0.05*	23.2±2.2 *NS*

Figure 2. Low Concentration of TG Induces Golgi Fragmentation Prior to UPR Through Elevated Cytosolic Ca^{2+}

(A) HeLa cells were treated with the indicated concentrations of TG for 20 min and stained for GM130. Scale bar, 20 μm.

(B) Quantitation of cells with fragmented Golgi in (A).

(C) Cells treated with TG as in (A) were analyzed by Western blots.

(D and E) Quantitation of p-eIF2α/eIF2α and Bip in (C) from five independent experiments.

(F) BAPTA-AM inhibits TG-induced Golgi fragmentation. HeLa cells treated with 100 nM TG for indicated times with or without 60 μM BAPTA-AM (B/AM) and stained for GM130. Scale bar, 20 μm.

(G) Quantitation of (F) from three independent experiments. Statistical analyses were performed using two-tailed Student's t tests (*, $p \leq 0.05$; **, $p \leq 0.01$; ***, $p \leq 0.001$).

(H) Electron micrographs of Golgi profiles in HeLa cells treated with 250 nM TG and B/AM for 20 min. Note that the Golgi is comprised of bulbous saccules in the TG-treatment, whereas in the B/AM pretreated cells the cisternae appear straight and well-stacked. Asterisks (*) indicate nuclei. Scale bar, 0.5 μm.

(I) Quantitation of the morphological features of Golgi stacks on the EM images in (H). For statistics, B/AM and TG were compared with DMSO treatment, whereas TG + B/AM was compared with TG treatment.

TG-Induced Golgi Fragmentation Increases Protein Trafficking in the Golgi

As GRASP-depletion-mediated Golgi destruction affects Golgi functions such as protein trafficking (Ahat et al., 2019b; Xiang et al., 2013), we examined the effect of TG treatment on the trafficking of the vesicular stomatitis virus glycoprotein (VSV-G) using the well-established RUSH system (Boncompain et al., 2012).

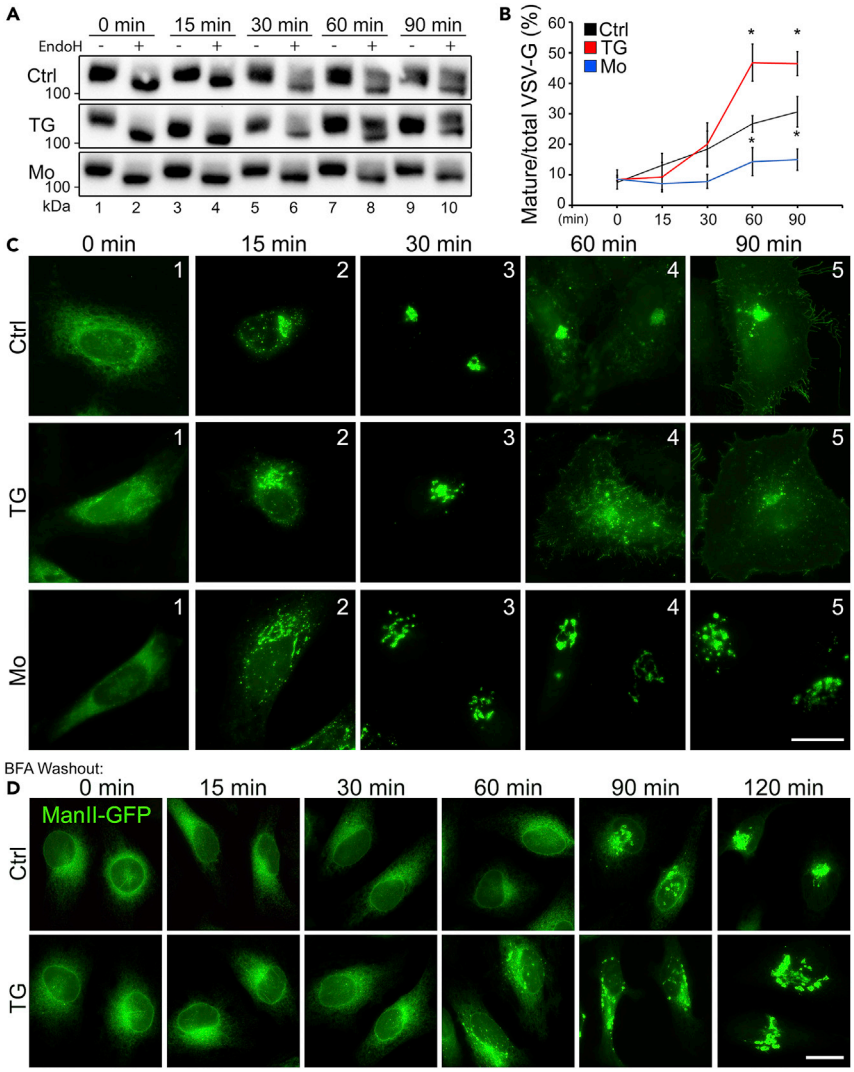

Figure 3. TG-Induced Golgi Fragmentation Has Minor Effect on Protein Trafficking

(A) Cells were transfected with the Str-Ii_VSVG wt-SBP-EGFP plasmid for 16 h followed by a 30-min treatment with DMSO, 250 nM TG, or 10 μM monensin (Mo) at 37°C. Cells were then incubated with complete medium containing 40 μM biotin (chase) for the indicated times, lysed and treated with (+) or without (–) EndoH, and analyzed by Western blot for GFP.

(B) Quantification of (A) for the percentage of EndoH-resistant VSV-G from three independent experiments. Quantitation results are shown as Mean ± SEM. Statistical analyses were performed using two-tailed Student's *t*-tests by comparing with the control (*$p \leq 0.05$).

(C) Representative images of (A) showing the subcellular localization of VSVG-EGFP at indicated time points after biotin chase. Scale bar, 20 μm.

(D) Fluorescent images showing the subcellular localization of ManII-GFP in cells treated with DMSO (Ctrl) or 250 nM TG at the indicated time points of BFA washout. ManII-GFP appears in the Golgi area beginning at 60 min, whereas this takes longer in control cells. Scale bar, 20 μm.

Cells were transfected with a plasmid that encodes both the invariant chain of the major histocompatibility complex (Ii, an ER protein) fused to core streptavidin and VSV-G fused to streptavidin-binding peptide (SBP). Under growth conditions without biotin, the interaction between streptavidin and SBP retains VSV-G in the ER. Upon the addition of biotin, this interaction is disrupted, resulting in synchronous release of the VSV-G reporter from the ER to the Golgi. Because VSV-G is a glycoprotein, we used endoglycosidase H (EndoH) to distinguish its core (ER and *cis* Golgi) and complex (*trans* Golgi and post-Golgi) glycosylation forms as an indicator of trafficking. As shown in Figure 3A, TG treatment first slightly decreased VSV-G trafficking at 15-min release but then increased VSV-G trafficking at 60 and 90 min compared with DMSO

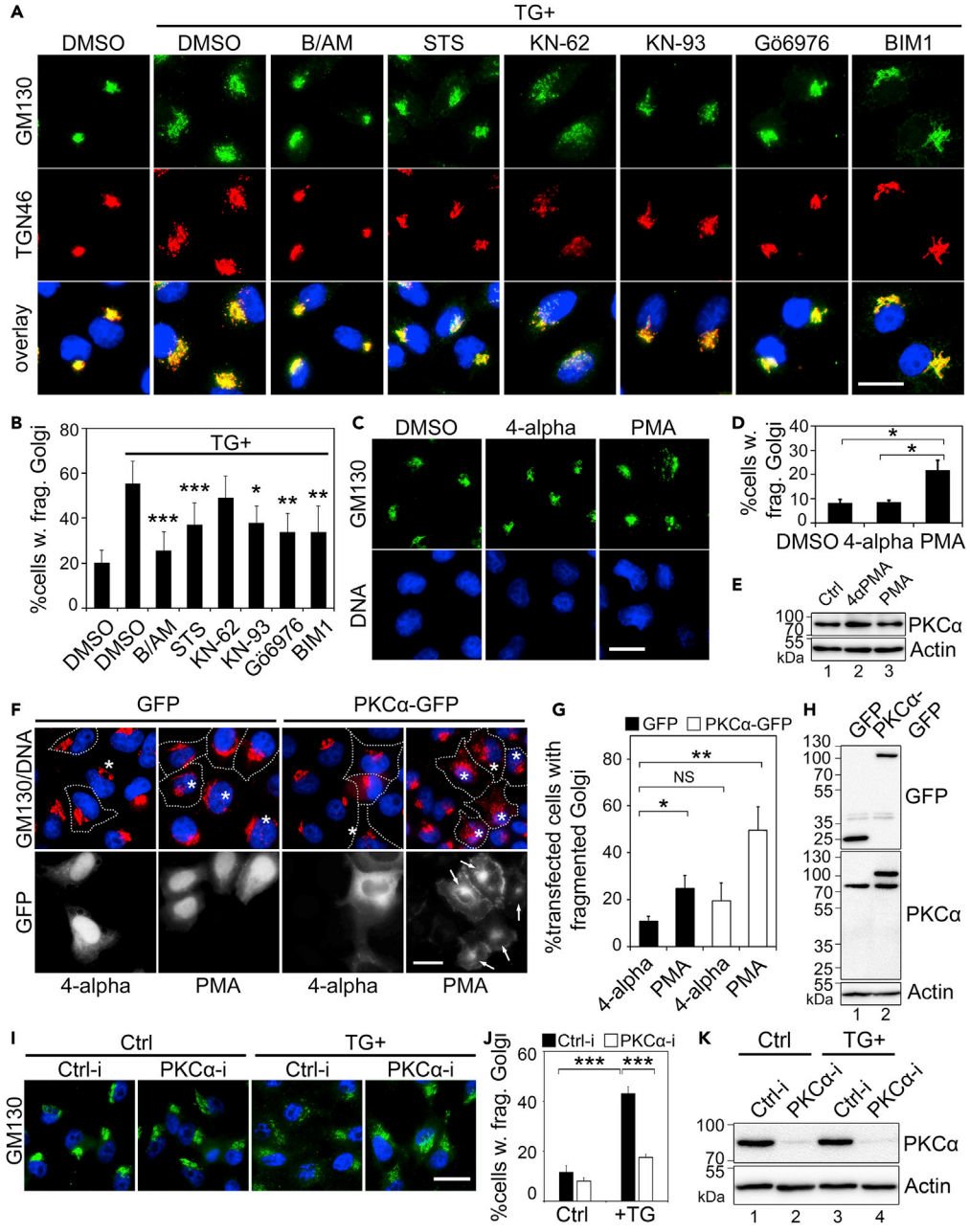

Figure 4. TG induces Golgi Fragmentation through PKCα

(A) Inhibition of PKC reduces TG-induced Golgi fragmentation. HeLa cells were pre-treated with DMSO, BAPTA-AM (B/AM, 60 μM for 10 min), staurosporine (STS, general kinase inhibitor, 2 μM for 10 min), KN-62 or KN-93 (CAMKII inhibitors, 10 μM and 5 μM, respectively, 10 min), or BIM1 or Gö6976 (PKC inhibitors, 2 μM and 4 μM, respectively, 10 min), and then with 250 nM TG for 20 min followed by immunostaining of GM130 and TGN46. Scale bar, 20 μm.

(B) Quantitation of cells in (A) with fragmented Golgi based on the GM130 pattern in the cell.

(C) HeLa cells were treated with 100 nM PMA for 1 h; 4-alpha-PMA of the same concentration was used as a control. Scale bar, 20 μm.

(D) Quantitation of cells with fragmented Golgi in (C).

(E) Cells treated as in (C) were analyzed by Western blot to show that PMA treatment does not change the PKCα expression level.

(F) Activation of ectopically expressed PKCα triggers its Golgi localization (indicated by "→") and Golgi fragmentation (*). Cells transfected with GFP or PKCα-GFP were treated with 100 nM PMA or 4-alpha for 1 h. Note the fragmented Golgi in these cells upon PMA treatment. Scale bar, 20 μm.

Figure 4. *Continued*

(G) Quantitation of cells in (F) with fragmented Golgi.

(H) Western blot of cells from (F) showing that ectopic PKC expression does not alter the endogenous PKCα expression level.

(I) HeLa cells were transfected with control (Ctrl-i) or PKC-specific siRNA for 48 h and then treated with 250 nM TG for 20 min. Cells were fixed and stained for GM130 (green) to show the Golgi structure. Scale bar, 20 μm.

(J) Quantitation of Golgi fragmentation of cells in (I).

(K) Cells in (I) were blotted for endogenous PKCα to evaluate the siRNA knockdown efficiency.

All quantitation results are shown as Mean ± SEM from three independent experiments. Statistical analyses were performed using two-tailed Student's *t*-tests (*$p \leq 0.05$; **$p \leq 0.01$; ***$p \leq 0.001$; NS, non-significant).

control. Our previous studies showed that VSV-G reaches the cis Golgi at 15–20 min and *trans* Golgi at ~90 min (Bekier et al., 2017; Li et al., 2019b). These results suggest that TG treatment may delay VSV-G release possibly by slowing down its folding; but once it reaches the cis Golgi, VSV-G trafficking across the Golgi stack is significantly accelerated. Monensin (Mo) is known to disrupt the Golgi structure and blocks TGN exit (Fliesler and Basinger, 1987) and thus was used as a control. As expected, monensin treatment resulted in VSV-G accumulation in the Golgi (Figures 3A–3C).

To confirm these results using an alternative approach, we treated cells with Brefeldin A (BFA) to accumulate ManII-GFP in the ER. We then washed out BFA and analyzed ManII-GFP in ER-to-Golgi trafficking. The results showed that ManII-GFP started to accumulate in the Golgi at 60 min of BFA washout in the presence of TG, whereas the same observation occurred at 90 min in the control (Figure 3D).

TG Induces Golgi Fragmentation Through PKCα Activation

Given that phosphorylation of Golgi structural proteins has been shown to cause Golgi fragmentation in physiological conditions such as in mitosis (Tang et al., 2010; Wang et al., 2003; Xiang and Wang, 2010), as well as in pathological conditions such as in Alzheimer disease (Joshi et al., 2014), we explored the possibility that phosphorylation of Golgi structural proteins may play a role in TG-induced Golgi fragmentation. We treated cells with staurosporine, a non-selective kinase inhibitor, and a number of specific inhibitors of calcium-related kinases such as protein kinase Cs (PKCs) and Ca^{2+}/calmodulin-dependent protein kinases (CAMKs). As shown in Figures S5C and S5D, staurosporine significantly reduced Golgi fragmentation in TG-treated cells. In addition, Bisindolylmaleimide I (BIM1), a selective PKC inhibitor, and KN-93, an inhibitor of CAMKII, also partially reduced Golgi fragmentation in TG-treated cells, whereas the myosin light-chain kinase inhibitor ML-7 and the protein kinase A (PKA) inhibitors H-89 and PKI had no such effects (Figures 4A, 4B, S5C, and S5D). These results suggest that either PKC and/or CAMKII is involved in TG-induced Golgi fragmentation. Because both BIM1 and KN-93 inhibitors have pleiotropic effects, we selected two alternative drugs, Gö6976 and KN-62, to inhibit PKC and CAMKII, respectively. Although Gö6976 inhibited TG-induced Golgi fragmentation effectively, KN-62 had no effect (Figures 4A and 4B), suggesting a major role of PKC in TG-induced Golgi fragmentation.

To further confirm that PKC activation causes Golgi fragmentation, we treated cells with phorbol 12-myristate 13-acetate (PMA), a widely used PKC activator, and its inactive enantiomer, 4-alpha-phorbol myristate acetate (4-alpha). The results showed that 4-alpha had no effect on the Golgi structure, whereas PMA treatment caused Golgi fragmentation (Figures 4C and 4D), although 4-alpha and PMA had no effect on the level of PKC expression (Figure 4E). In addition, expression of CAMKIIβ had no effect on the Golgi morphology (Figures S5E and S5F). There have been reports that activation of MAPK/ERK or PKD signaling causes Golgi fragmentation (Jamora et al., 1999; Jesch et al., 2001), we therefore inhibited these two kinases with U0126 or H-89, respectively. Pre-treatment of cells with these kinase inhibitors did not prevent Golgi fragmentation upon the addition of TG (Figures S5G and S5H). Taken together, these results indicate that TG induces Golgi fragmentation through PKC activation.

PKC has multiple isoforms including α, βI, βII, γ, δ, ϵ, η, ζ, and ι (Kajimoto et al., 2001). To identify the PKC isoform responsible for TG-induced Golgi fragmentation, we expressed GFP-tagged PKC isoforms, including all four known classical PKC (cPKC) isoforms (α, βI, βII, γ) that respond to Ca^{2+} stimuli, one from the non-calcium responsive novel PKC (nPKC, δ) and one from the atypical PKC (nPKC, ζ) subfamily (Figures S6A and S6B). To enhance the activity of expressed PKC, we also treated cells with PMA, using 4-alpha as a control. The results showed that expression of PKCα and treatment of cells with PMA increased Golgi fragmentation (Figures 4F–4H, S6A, and S6B). Interestingly, in addition to the localization to the

plasma membrane as previously reported (Becker and Hannun, 2003), wild-type PKCα-GFP was also concentrated on the Golgi upon PMA treatment, as indicated by the colocalization with GM130 (Figures 4F and S6B), whereas other PKC isoforms, or the inactive PKCα K368R mutant (Baier-Bitterlich et al., 1996), did not show the same phenotype (Figures 4F and S6B–S6D). To further specify that PKCα mediates TG-induced Golgi fragmentation, we knocked down PKCα in cells with siRNA. The results showed that PKCα depletion reduces Golgi fragmentation after TG treatment (Figures 4I–4K). Taken together, these results demonstrate that PKCα activation causes Golgi fragmentation.

PKCα Induces Golgi Fragmentation Through GRASP55 Phosphorylation

Because activated PKCα localizes to the Golgi, we thought it might phosphorylate Golgi structural proteins. To identify potential PKCα targets on the Golgi, we performed gel mobility shift assays on a number of Golgi structural proteins, tethering factors, and SNARE proteins after TG treatment (Figure S6E). To ensure that the band shift was caused by phosphorylation, we also applied staurosporine (2 μM for 10 min prior to TG treatment) to TG-treated cells to broadly inhibit phosphorylation. Among the proteins tested, GRASP55 and GRASP65 showed a smear above the main bands (Figure S6E), indicating a partial phosphorylation of the proteins. To increase the resolution of phosphorylated proteins we utilized phos-tag gels, which showed GRASP55, but not GRASP65, to be significantly shifted up after TG treatment (250 nM, 1 h) (Figure S6F). TG-induced mobility shift of GRASP55 was not seen upon Tm treatment (Figure 5A, lanes 2 vs. 3) and was less dramatic than that by nocodazole (Noc) treatment that blocks cells in mitosis when GRASP55 is fully phosphorylated (Figure 5A, lanes 3 vs. 4) (Xiang and Wang, 2010), indicating that TG induced partial phosphorylation of GRASP55. The mobility shift of GRASP55 triggered by TG treatment was abolished by the addition of staurosporine (Figure 5C, lanes 4 vs. 3; Figure S6F, lanes 3 vs. 2), validating the mobility shift by phosphorylation. In addition, incubation of purified recombinant GRASP55 with purified PKCα caused GRASP55 phosphorylation, confirming that PKCα can directly phosphorylate GRASP55 (Figure 5D). In this experiment, PKCα was also autophosphorylated (Figure 5D). Taken together, these results demonstrate that TG treatment activates PKCα, which subsequently phosphorylates GRASP55.

GRASP55 contains an N-terminal GRASP domain that forms dimers and oligomers and a C-terminal SPR domain with multiple phosphorylation sites (Xiang and Wang, 2010; Zhang and Wang, 2015). To map the PKCα phosphorylation site on GRASP55, we expressed GFP-tagged GRASP55 truncation mutants (Zhang et al., 2018), treated the cells with TG, and determined their phosphorylation. A visible mobility shift of the GRASP55 variants was observed on the mutants possessing amino acids (aa)251-300 but not the truncated forms shorter than aa250 (Figures 5E and 5F). To further determine the functional consequence of GRASP55 phosphorylation, we expressed these constructs and treated cells with or without TG. The exogenously expressed GRASP55 truncation mutants were targeted to the Golgi as indicated by giantin as a Golgi marker but had no impact on the Golgi structure (Figure S6G). However, when cells were treated with TG, expression of the N-terminal aa250 or shorter reduced TG-induced Golgi fragmentation, whereas expression of N-terminal aa300 or longer had no significant effect (Figures 5G and 5H). These results demonstrated that phosphorylation of GRASP55 within aa251-300 is important for TG-induced Golgi fragmentation.

Histamine Modulates the Golgi Structure Through the Same Pathway as TG Treatment

It is known that histamine activates Ca^{2+}-dependent PKC isoforms and upregulates cytokine secretion via the release of calcium from the ER into the cytosol (Matsubara et al., 2005). It has also been shown that histamine triggers protein secretion and Golgi fragmentation (Saini et al., 2010), but the underlying mechanism has not been revealed. Therefore, we treated HeLa cells with histamine and determined the effect on Golgi morphology. As shown in Figures 6A and 6B, histamine treatment induced Golgi fragmentation in a dose- and time-dependent manner. More than 40% of cells possessed fragmented Golgi after 100 μM histamine treatment for 1 h, a concentration and time often used in previous studies (Sahoo et al., 2017; Xie et al., 2018). Subsequent EM analysis confirmed that histamine treatment induced alterations in the Golgi structure, including fewer cisternae per stack, shorter cisternae, and an increased number of Golgi-associated vesicles (Figures 6C, 6D, and S7A).

It has been previously shown that histamine activates Gβγ, which causes TGN fragmentation (Saini et al., 2010). Because HeLa cells do not express Gβγ, and histamine treatment triggers fragmentation of the entire Golgi stack (Figures 6C and 6D), the Golgi fragmentation observed in our study may occur through a different mechanism. Indeed, as TG, histamine-induced Golgi fragmentation also depended on PKC, as the addition of the PKC inhibitor Gö6976 reduced histamine-induced Golgi fragmentation (Figures 6E and

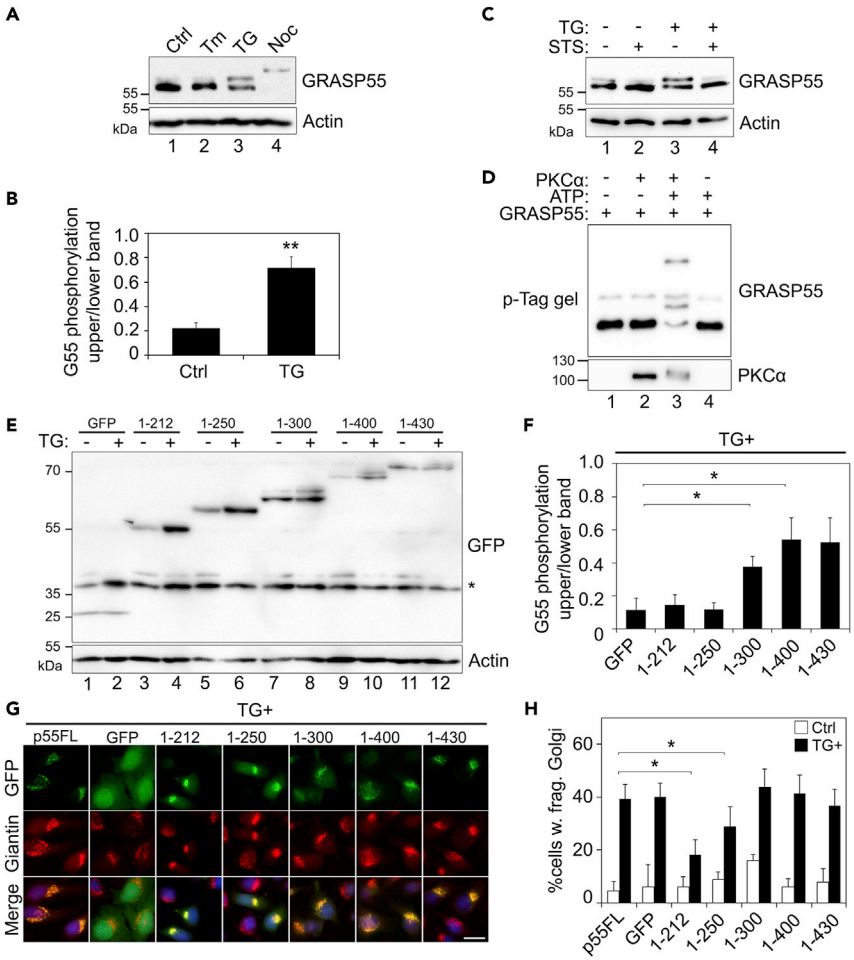

Figure 5. TG Induces Golgi Fragmentation through GRASP55 Phosphorylation

(A) GRASP55 is phosphorylated upon TG treatment. HeLa cells treated with Tm, TG, or nocodazole (Noc) were analyzed by phos-tag gels and Western blot. Note the mobility shift of GRASP55 upon TG treatment compared with control (Ctrl). Nocodazole-arrested mitotic cells were used as a positive control for GRASP55 phosphorylation.

(B) TG-induced GRASP55 mobility shift is abolished by kinase inhibition. Cells were pre-treated with 2 μM staurosporine (STS) for 10 min and then with 250 nM TG for 1 h followed by analysis with phos-tag gels and Western blot.

(C) Quantitation of GRASP55 phosphorylation in TG-treated cells. The intensity of the phosphorylated (upper) band was quantified by densitometry analysis and plotted relative to the intensities of the full length (lower) band. Shown are the results of relative phosphorylation of GRASP55 from three independent experiments.

(D) PKCα phosphorylates GRASP55 *in vitro*. Purified PKCα and GRASP55 were incubated in a kinase buffer with or without ATP as indicated and analyzed by phos-tag gels and Western blot for GRASP55 and PKCα.

(E) Mapping the phosphorylation site on GRASP55 by expressing GRASP55 truncation mutants. Indicated GFP-tagged GRASP55 constructs were expressed in HeLa cells. After TG treatment, GRASP55 was analyzed by mobility shift as in (A). Note the mobility shift in lanes 8, 10, and 12.

(F) Quantitation of GRASP55 phosphorylation in TG-treated cells from (E).

(G) TG-induced Golgi fragmentation is rescued by the expression of non-phosphorylatable GRASP55 proteins. Cells expressing the indicated GRASP55 constructs were stained for giantin. Scale bar, 20 μm.

(H) Quantitation of cells in (G) with fragmented Golgi. Results are shown as Mean ± SEM.

Statistical analyses were performed using two-tailed Student's *t*-tests (*$p \leq 0.05$; **$p \leq 0.01$).

6F). To investigate the functional consequence of histamine treatment on Golgi function, VSV-G trafficking experiments were performed as above. As shown in Figures S7B and S7C, histamine treatment slightly decreased VSV-G trafficking within 45-min release but then began to increase the trafficking speed in the Golgi at later time points. These results demonstrate that histamine treatment affects Golgi structure and function through a similar mechanism as TG.

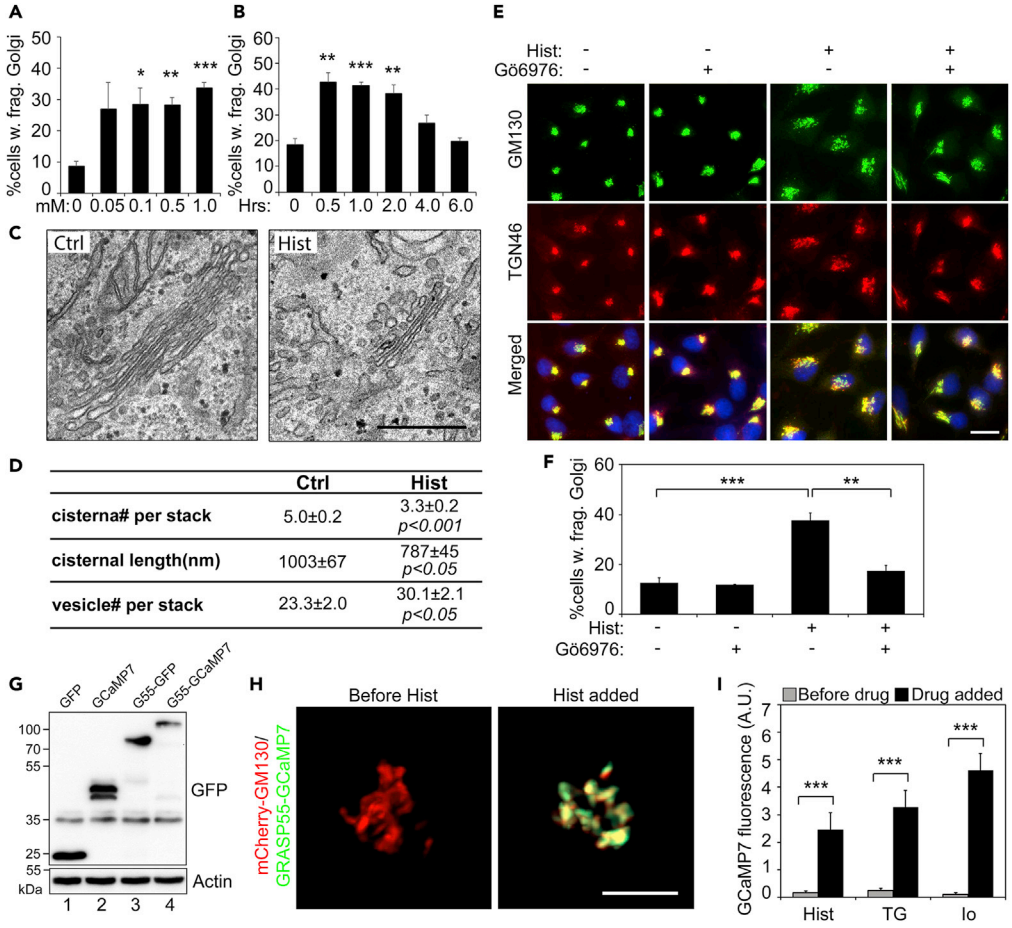

Figure 6. Histamine Induces Golgi Fragmentation through PKC Activation

(A) HeLa cells were treated with indicated concentrations of histamine for 1 h, stained for GM130, and quantified for the percentage of cells with fragmented Golgi. Shown are the quantitation results.

(B) HeLa cells were treated with 100 μM histamine for the indicated times and analyzed as in (A). Note that histamine induced Golgi fragmentation within 2 h.

(C) Electron micrographs of Golgi profiles in HeLa cells treated with DMSO control (Ctrl, left panel) or 100 μM histamine for 1 h (right panel). Note the reduced size of the Golgi in histamine-treated cells. Scale bar, 0.5 μm.

(D) Quantitation of the morphological features of the Golgi stacks in (C). For statistics, histamine treated cells were compared with control cells.

(E) Cells were pre-treated with (+) or without (−) the PKC inhibitor Gö6976 at 37°C for 10 min followed by the addition of 100 μM histamine for 60 min. Scale bar, 20 μm.

(F) Quantitation of cells with fragmented Golgi in (E).

(G) Expression of the GRASP55-GCaMP7 Golgi Ca^{2+} sensor. HeLa cells transfected with indicated proteins were analyzed by Western blot for GFP.

(H) Histamine treatment increases the GRASP55-GCaMP7 signal. HeLa cells were co-transfected with mCherry-GM130 (red) and GRASP55-GCAMP7 (green). Shown are still frames before (left panel) or after (right) histamine was added. Scale bar, 5 μm.

(I) TG and ionomycin treatments increase the GRASP55-GCaMP7 signal. HeLa cells expressing GRASP55-GCaMP7 were treated with 100 μM histamine (Hist), 250 nM TG, or 1 μM ionomycin (Io) for 1 h. Shown are the quantitation of the fluorescence intensity before and after the drug was added.

All quantitation results are shown as Mean ± SEM. Statistical analyses were performed using two-tailed Student's *t*-tests (*$p \leq 0.05$; **$p \leq 0.01$; ***$p \leq 0.001$).

Although it has been well documented that TG or histamine treatment elevates Ca^{2+} level in the cytosol, whether this is also true for the Ca^{2+} level in the Golgi region has not been reported. To test the effect of TG or histamine treatment on the Ca^{2+} level in the Golgi region in real time, we fused the Ca^{2+} probe GCaMP (Muto et al., 2013) to GRASP55, expressed the GRASP55-GCaMP construct in cells (Figure 6G), and performed live cell imaging.

Treatment of cells with 100 μM histamine caused a robust calcium spike (Figure 6H; Video S1). Subsequent experiments using this novel Golgi-localized Ca^{2+} probe demonstrated that treatment of cells with TG and Io also significantly elevated the Ca^{2+} level in the Golgi (Figure 6I). Taken together, our results demonstrated that histamine or TG treatment elevates the Ca^{2+} level in the Golgi region, which subsequently activates PKCα, leading to GRASP55 phosphorylation and Golgi fragmentation. Thus, this study revealed a novel mechanism of how histamine, and perhaps other drugs, modulates Golgi structure and function.

DISCUSSION

In this study, by comparing Golgi fragmentation with ER stress in response to TG, Tm, and DTT treatments, we uncovered a novel signaling pathway through which increased cytosolic Ca^{2+} triggers Golgi fragmentation through PKCα activation and GRASP55 phosphorylation. Significantly, we also demonstrated that histamine modulates the Golgi structure and function via a similar mechanism, which opens a new window through which we can better understand the effect of histamine on cell physiology.

One possible model of Golgi stress is that the expanding capacity of the ER during cellular stress leads to the failure of the Golgi as it is over-burdened with misfolded or improperly folded proteins, affecting its functions such as glycosylation (Oku et al., 2011). However, our results do not support this hypothesis for two reasons. First, although three ER stress inducers, TG, Tm, and DTT, all induce ER stress, only TG treatment causes Golgi fragmentation. Second, TG induces Golgi fragmentation at a low dose and time when UPR is undetectable. These results demonstrate that Golgi fragmentation occurs independently of ER stress, perhaps via the modification of pre-existing cellular materials. Therefore, the Golgi may possess its own mechanism to sense and respond to stress alongside or completely separate from the ER. Furthermore, our study revealed a novel mechanism that coordinates Golgi structure and perhaps function: TG treatment increases cytoplasmic Ca^{2+}, which activates PKCα, which subsequently phosphorylates GRASP55, impairing its function in Golgi structure formation. GRASP55 therefore provides the conceptual link between an extracellular cue and Golgi morphological change during stress.

GRASP55 is comprised of an N-terminal GRASP domain (aa1-212) that forms dimers and oligomers and functions as a membrane tether to maintain an intact Golgi structure and an SPR domain (aa212-454) that undergoes post-translational modifications and functions as the regulatory domain of the protein (Xiang and Wang, 2010; Zhang and Wang, 2015). Originally, GRASP55 was found to be phosphorylated by ERK2 at T225 and T222 (Jesch et al., 2001). Subsequently, additional sites, such as S245 and T249, were identified to be phosphorylated in mitosis, which is required for mitotic Golgi disassembly (Xiang and Wang, 2010). Recently, GRASP55 was discovered to be de-O-GlcNAcylated upon energy or nutrient deprivation and regulates autophagosome maturation (Zhang et al., 2018, 2019). These results indicate that GRASP55 is an excellent candidate to function as both a sensor and effector of cellular stresses. Thus, GRASP55 is likely a master regulator of Golgi structure formation, function, and stress responses.

Our *in vitro* kinase assay demonstrated that PKCα can directly phosphorylate GRASP55 likely on more than one site. The mobility shift of GRASP55 observed in cells consisted of only one obvious band, whereas the *in vitro* experiment showed two clear bands, suggesting that phosphorylation of GRASP55 in cells might occur less frequently. Using GRASP55 truncation mutants we mapped the site(s) of PKC-mediated phosphorylation to the aa251-300 region. Expression of truncation mutants of GRASP55 that lack this region significantly reduced TG-induced Golgi fragmentation. Previously, it has been shown by mass spectrometry that GRASP55 is phosphorylated on S441 after TG treatment, but the kinase mediating this phosphorylation is unknown (Gee et al., 2011). Although our results are consistent with this previous study, the exact phosphorylation site(s) need further investigation.

Histamine is a neuroendocrine hormone involved in the regulation of stomach acid secretion, brain function, and immune response; many of these functions involve secretion (Karpati et al., 2018; Sahoo et al., 2017; Xie et al., 2018). The role of histamine in immune response is often through the activation of the downstream kinase PKCα. For example, histamine enhances the secretion of granulocyte-macrophage colony stimulation factor (GM-CSF) and nerve growth factor (NGF) in different cell types, both through a PKCα-dependent mechanism (Sohen et al., 2001). Interestingly, histamine promotes HeLa cell proliferation and growth and has been shown to be elevated in cancers where Golgi is fragmented and secretion is enhanced. In our experiments, histamine induced a clear Golgi fragmentation phenotype, confirming a link between histamine and Golgi fragmentation. Additionally, expression of PKCα, but not other PKC

isoforms, along with a stimulation with PMA, exhibited an additive Golgi fragmentation effect. Consistent with prior work showing that disassembly of Golgi stacks accelerates protein trafficking (Xiang et al., 2013), our findings therefore offer a mechanism for how histamine increases secretion of inflammatory factors.

How Ca^{2+} controls membrane trafficking at the plasma membrane has been well documented in regulated secretion in specific cell types such as neurons, neuroendocrine cells, and mast cells, whereas its role in other cell types is less well known. Ca^{2+} dynamic at the Golgi as well as its role in membrane trafficking at the Golgi is still an understudied area. There are EF-hand Ca^{2+} binding proteins associated in the Golgi. For example, Cab45 is located in the Golgi lumen, whereas Calnuc is found in both cell cytosol and membrane fractions (Lin et al., 1998). At the cis-Golgi, Calnuc binds Gαi and Gαs, which is thought to be important for vesicular trafficking (Lin et al., 2000). There are also P-Type ATPases (SPCAs) such as SPCA1 located in the Golgi that regulate Ca^{2+} homeostasis in the Golgi and control neural polarity (Sepulveda et al., 2009; Vanoevelen et al., 2007). Our study provided a novel link between thapsigargin and histamine treatment, elevation of Ca^{2+} concentration in the Golgi region, activation of PKC and phosphorylation of Golgi GRASP55, and modification of Golgi structure and function.

Our study revealed that TG induces Golgi fragmentation through increasing cytosolic Ca^{2+} and GRASP55 phosphorylation. A similar case has been described previously in Alzheimer disease, where cytosolic calcium increases by Aβ treatment triggers activation of a cytosolic protease, calpain, which cleaves p35 to generate p25 and activate Cdk5, a cytoplasmic kinase that is highly expressed in neurons (Lew et al., 1994). Subsequently, activated Cdk5 phosphorylates GRASP65 and perhaps other Golgi structural proteins, leading to Golgi fragmentation (Joshi et al., 2014, 2015). Although PKC and GRASP55 were not the focus in this study, expression of a phosphorylation-deficient mutant of GRASP55 significantly reduced Golgi fragmentation as well as Aβ production. Taken together, our studies indicate that the Golgi is sensitive to cellular stimuli and stresses as in disease conditions,and responds to signaling cues to adjust its structure and function through increasing cytosolic Ca^{2+} and GRASP55 modification. Future studies defining the detailed mechanisms may help understand disease pathologies with Golgi and trafficking defects.

Limitations of the Study

Phosphorylation occurs more frequently *in vitro* than in cells. The exact phosphorylation site(s) on GRASP55 needs further investigation.

METHODS

All methods can be found in the accompanying Transparent Methods supplemental file.

DATA AND CODEAVAILABILITY

All data from this study is available upon request.

SUPPLEMENTAL INFORMATION

Supplemental Information can be found online at https://doi.org/10.1016/j.isci.2020.100952.

ACKNOWLEDGMENTS

We thank Drs. Mohammed Akaaboune, Peter Arvan, Hesham El-Shewy, Yusuf Hannun, Isabel Martinez Peña, Franck Perez, Joachim Seemann, Haoxing Xu, and Kezhong Zhang for reagents; Drs. Peter Blumberg, John Kuwada, Edward Stuenkel, and Haoxing Xu for technical assistance; Gregg Sobocinski, Dana Holcomb, Miles McKenna, and Edwin De Feijter for microscope and equipment expertise. This work was supported by the National Institutes of Health (Grants GM112786, GM105920, and GM130331), MCubed and the Fastforward Protein Folding Disease Initiative of the University of Michigan to Y.W.. S.I. is a graduate student who has been partially supported by the Mary Sue and Kenneth Coleman Endowed Fellowship Fund from the University of Michigan. Many thanks to past and current members of the Wang lab, including Erpan Ahat, Michael Bekier, Shijiao Huang, Courtney Killeen, Haoran Huang, and Ron Benyair.

AUTHOR CONTRIBUTIONS

Conception and design: S. R., S. I., and Y. W.

Development of methodology: S. I., S. R., X. Z., J. Z., J. L., and Y. W.

Acquisition of data: S. I., S. R., M. F., X. Z., J. Z., and D. E.

Analysis and interpretation of data: S. I., S. R., M. F., and Y. W.

Writing, review, and/or revision of the manuscript: S. I., and Y. W.

Administrative, technical, or material support: S. I., and Y. W.

Study supervision: Y. W.

DECLARATION OF INTERESTS

The authors declare no competing financial interests.

Received: October 28, 2019
Revised: January 31, 2020
Accepted: February 25, 2020
Published: March 27, 2020

REFERENCES

Ahat, E., Li, J., and Wang, Y. (2019a). New insights into the Golgi stacking proteins. Front. Cell Dev. Biol. *7*, 131.

Ahat, E., Xiang, Y., Zhang, X., Bekier, M.E., and Wang, Y. (2019b). GRASP depletion-mediated Golgi destruction decreases cell adhesion and migration via the reduction of alpha5beta1 integrin. Mol. Biol. Cell *30*, 766–777.

Baier-Bitterlich, G., Uberall, F., Bauer, B., Fresser, F., Wachter, H., Grunicke, H., Utermann, G., Altman, A., and Baier, G. (1996). Protein kinase C-theta isoenzyme selective stimulation of the transcription factor complex AP-1 in T lymphocytes. Mol. Cell Biol. *16*, 1842–1850.

Becker, K.P., and Hannun, Y.A. (2003). cPKC-dependent sequestration of membrane-recycling components in a subset of recycling endosomes. J. Biol. Chem. *278*, 52747–52754.

Bekier, M.E., 2nd, Wang, L., Li, J., Huang, H., Tang, D., Zhang, X., and Wang, Y. (2017). Knockout of the Golgi stacking proteins GRASP55 and GRASP65 impairs Golgi structure and function. Mol. Biol.Cell *28*, 2833–2842.

Boncompain, G., Divoux, S., Gareil, N., de Forges, H., Lescure, A., Latreche, L., Mercanti, V., Jollivet, F., Raposo, G., and Perez, F. (2012). Synchronization of secretory protein traffic in populations of cells. Nat. Methods *9*, 493–498.

Chen, D., Purohit, A., Halilovic, E., Doxsey, S.J., and Newton, A.C. (2004). Centrosomal anchoring of protein kinase C betaII by pericentrin controls microtubule organization, spindle function, and cytokinesis. J. Biol. Chem. *279*, 4829–4839.

Cooke, M., Magimaidas, A., Casado-Medrano, V., and Kazanietz, M.G. (2017). Protein kinase C in cancer: the top five unanswered questions. Mol. Carcinog. *56*, 1531–1542.

El Homasany, B.S.E.D., Volkov, Y., Takahashi, M., Ono, Y., Keryer, G., Delouvee, A., Looby, E., Long, A., and Kelleher, D. (2005). The scaffolding protein CG-NAP/AKAP450 is a critical integrating component of the LFA-1-induced signaling complex in migratory T cells. J. Immunol. *175*, 7811–7818.

Farhan, H., Wendeler, M.W., Mitrovic, S., Fava, E., Silberberg, Y., Sharan, R., Zerial, M., and Hauri, H.P. (2010). MAPK signaling to the early secretory pathway revealed by kinase/phosphatase functional screening. J. Cell Biol. *189*, 997–1011.

Feinstein, T.N., and Linstedt, A.D. (2008). GRASP55 regulates Golgi ribbon formation. Mol. Biol.Cell *19*, 2696–2707.

Fliesler, S.J., and Basinger, S.F. (1987). Monensin stimulates glycerolipid incorporation into rod outer segment membranes. J. Biol. Chem. *262*, 17516–17523.

Fujita, Y., and Okamoto, K. (2005). Golgi apparatus of the motor neurons in patients with amyotrophic lateral sclerosis and in mice models of amyotrophic lateral sclerosis. Neuropathology *25*, 388–394.

Gee, H.Y., Noh, S.H., Tang, B.L., Kim, K.H., and Lee, M.G. (2011). Rescue of DeltaF508-CFTR trafficking via a GRASP-dependent unconventional secretion pathway. Cell *146*, 746–760.

Gonatas, N.K., Gonatas, J.O., and Stieber, A. (1998). The involvement of the Golgi apparatus in the pathogenesis of amyotrophic lateral sclerosis, Alzheimer's disease, and ricin intoxication. Histochem. Cell Biol. *109*, 591–600.

Griner, E.M., and Kazanietz, M.G. (2007). Protein kinase C and other diacylglycerol effectors in cancer. Nat. Rev. Cancer *7*, 281–294.

Hilditch-Maguire, P., Trettel, F., Passani, L.A., Auerbach, A., Persichetti, F., and MacDonald, M.E. (2000). Huntingtin: an iron-regulated protein essential for normal nuclear and perinuclear organelles. Hum. Mol. Genet. *9*, 2789–2797.

Ito, Y., Takeda, Y., Seko, A., Izumi, M., and Kajihara, Y. (2015). Functional analysis of endoplasmic reticulum glucosyltransferase (UGGT): synthetic chemistry's initiative in glycobiology. Semin. Cell Dev. Biol. *41*, 90–98.

Jamora, C., Yamanouye, N., Van Lint, J., Laudenslager, J., Vandenheede, J.R., Faulkner, D.J., and Malhotra, V. (1999). Gbetagamma-mediated regulation of Golgi organization is through the direct activation of protein kinase D. Cell *98*, 59–68.

Jesch, S.A., Lewis, T.S., Ahn, N.G., and Linstedt, A.D. (2001). Mitotic phosphorylation of Golgi reassembly stacking protein 55 by mitogen-activated protein kinase ERK2. Mol. Biol. Cell *12*, 1811–1817.

Jones, K.T., and Sharpe, G.R. (1994). Thapsigargin raises intracellular free calcium levels in human keratinocytes and inhibits the coordinated expression of differentiation markers. Exp. Cell Res. *210*, 71–76.

Joshi, G., Bekier, M.E., 2nd, and Wang, Y. (2015). Golgi fragmentation in Alzheimer's disease. Front. Neurosci. *9*, 340.

Joshi, G., Chi, Y., Huang, Z., and Wang, Y. (2014). Abeta-induced Golgi fragmentation in Alzheimer's disease enhances Abeta production. Proc. Natl. Acad. Sci. U S A *111*, E1230–E1239.

Kajimoto, T., Ohmori, S., Shirai, Y., Sakai, N., and Saito, N. (2001). Subtype-specific translocation of the delta subtype of protein kinase C and its activation by tyrosine phosphorylation induced by ceramide in HeLa cells. Mol. Cell Biol. *21*, 1769–1783.

Karpati, A., Yoshikawa, T., Nakamura, T., Iida, T., Matsuzawa, T., Kitano, H., Harada, R., and Yanai, K. (2018). Histamine elicits glutamate release from

cultured astrocytes. J. Pharmacol. Sci. *137*, 122–128.

Kim, H., Zamel, R., Bai, X.H., and Liu, M. (2013). PKC activation induces inflammatory response and cell death in human bronchial epithelial cells. PLoS One *8*, e64182.

Krause, W.J. (2000). Brunner's glands: a Structural,Histochemical and pathological profile. Prog. Histochem. Cytochem. *35*, 255–367.

Lew, J., Huang, Q.Q., Qi, Z., Winkfein, R.J., Aebersold, R., Hunt, T., and Wang, J.H. (1994). A brain-specific activator of cyclin-dependent kinase 5. Nature *371*, 423–426.

Li, J., Ahat, E., and Wang, Y. (2019a). Golgi Structure and Function in Health, Stress and Diseases (Springer Nature).

Li, J., Tang, D., Ireland, S.C., and Wang, Y. (2019b). DjA1 maintains Golgi integrity via interaction with GRASP65. Mol. Biol. Cell *30*, 478–490.

Lin, P., Fischer, T., Weiss, T., and Farquhar, M.G. (2000). Calnuc, an EF-hand Ca(2+) binding protein, specifically interacts with the C-terminal alpha5-helix of G(alpha)i3. Proc. Natl. Acad. Sci. U S A *97*, 674–679.

Lin, P., Le-Niculescu, H., Hofmeister, R., McCaffery, J.M., Jin, M., Hennemann, H., McQuistan, T., De Vries, L., and Farquhar, M.G. (1998). The mammalian calcium-binding protein, nucleobindin (CALNUC), is a Golgi resident protein. J. Cell Biol. *141*, 1515–1527.

Matsubara, M., Tamura, T., Ohmori, K., and Hasegawa, K. (2005). Histamine H1 receptor antagonist blocks histamine-induced proinflammatory cytokine production through inhibition of Ca2+-dependent protein kinase C, Raf/MEK/ERK and IKK/I kappa B/NF-kappa B signal cascades. Biochem. Pharmacol. *69*, 433–449.

Mizuno, Y., Hattori, N., Kitada, T., Matsumine, H., Mori, H., Shimura, H., Kubo, S., Kobayashi, H., Asakawa, S., Minoshima, S., et al. (2001). Familial Parkinson's disease. Alpha-synuclein and parkin. Adv. Neurol. *86*, 13–21.

Mourelatos, Z., Gonatas, N.K., Stieber, A., Gurney, M.E., and Dal Canto, M.C. (1996). The Golgi apparatus of spinal cord motor neurons in transgenic mice expressing mutant Cu,Zn superoxide dismutase becomes fragmented in early, preclinical stages of the disease. Proc. Natl. Acad. Sci. U S A *93*, 5472–5477.

Muto, A., Ohkura, M., Abe, G., Nakai, J., and Kawakami, K. (2013). Real-time visualization of neuronal activity during perception. Curr. Biol. *23*, 307–311.

Nishizuka, Y. (1995). Protein kinase C and lipid signaling for sustained cellular responses. FASEB J. *9*, 484–496.

Oku, M., Tanakura, S., Uemura, A., Sohda, M., Misumi, Y., Taniguchi, M., Wakabayashi, S., and Yoshida, H. (2011). Novel cis-acting element GASE regulates transcriptional induction by the Golgi stress response. Cell Struct. Funct. *36*, 1–12.

Petrosyan, A., Holzapfel, M.S., Muirhead, D.E., and Cheng, P.W. (2014). Restoration of compact Golgi morphology in advanced prostate cancer enhances susceptibility to galectin-1-induced apoptosis by modifying mucin O-glycan synthesis. Mol. Cancer Res. *12*, 1704–1716.

Puthenveedu, M.A., Bachert, C., Puri, S., Lanni, F., and Linstedt, A.D. (2006). GM130 and GRASP65-dependent lateral cisternal fusion allows uniform Golgi-enzyme distribution. Nat. Cell Biol. *8*, 238–248.

Rambourg, A., Clermont, Y., Chretien, M., and Olivier, L. (1993). Modulation of the Golgi apparatus in stimulated and nonstimulated prolactin cells of female rats. Anat. Rec. *235*, 353–362.

Sahoo, N., Gu, M., Zhang, X., Raval, N., Yang, J., Bekier, M., Calvo, R., Patnaik, S., Wang, W., King, G., et al. (2017). Gastric acid secretion from parietal cells is mediated by a Ca(2+)efflux channel in the tubulovesicle. Dev.Cell *41*, 262–273 e266.

Saini, D.K., Karunarathne, W.K., Angaswamy, N., Saini, D., Cho, J.H., Kalyanaraman, V., and Gautam, N. (2010). Regulation of Golgi structure and secretion by receptor-induced G protein betagamma complex translocation. Proc. Natl. Acad. Sci. U S A *107*, 11417–11422.

Sepulveda, M.R., Vanoevelen, J., Raeymaekers, L., Mata, A.M., and Wuytack, F. (2009). Silencing the SPCA1 (secretory pathway Ca2+-ATPase isoform 1) impairs Ca2+ homeostasis in the Golgi and disturbs neural polarity. J. Neurosci. *29*, 12174–12182.

Sewell, R., Backstrom, M., Dalziel, M., Gschmeissner, S., Karlsson, H., Noll, T., Gatgens, J., Clausen, H., Hansson, G.C., Burchell, J., et al. (2006). The ST6GalNAc-I sialyltransferase localizes throughout the Golgi and Is responsible for the synthesis of the tumor-associated sialyl-Tn O-glycan in human breast cancer. J. Biol. Chem. *281*, 3586–3594.

Sohen, S., Ooe, H., Hashima, M., Nonaka, T., Fukuda, K., and Hamanishi, C. (2001). Activation of histamine H1 receptor results in enhanced proteoglycan synthesis by human articular chondrocyte: involvement of protein kinase C and intracellular Ca(2+). Pathophysiology *8*, 93–98.

Sutterlin, C., Polishchuk, R., Pecot, M., and Malhotra, V. (2005). The Golgi-associated protein GRASP65 regulates spindle dynamics and is essential for cell division. Mol. Biol.Cell *16*, 3211–3222.

Tan, X., Banerjee, P., Guo, H.F., Ireland, S., Pankova, D., Ahn, Y.H., Nikolaidis, I.M., Liu, X., Zhao, Y., Xue, Y., et al. (2016). Epithelial-to-mesenchymal transition drives a pro-metastatic Golgi compaction process through scaffolding protein PAQR11. J. Clin. Invest. *127*, 117–131.

Tang, D., and Wang, Y. (2013). Cell cycle regulation of Golgi membrane dynamics. Trends Cell Biol. *23*, 296–304.

Tang, D., Yuan, H., and Wang, Y. (2010). The role of GRASP65 in Golgi cisternal stacking and cell cycle progression. Traffic *11*, 827–842.

Tang, D., Yuan, H., Vielemeyer, O., Perez, F., and Wang, Y. (2012). Sequential phosphorylation of GRASP65 during mitotic Golgi disassembly. Biol. Open *1*, 1204–1214.

Thayer, D.A., Jan, Y.N., and Jan, L.Y. (2013). Increased neuronal activity fragments the Golgi complex. Proc. Natl. Acad. Sci. U S A *110*, 1482–1487.

Vanoevelen, J., Dode, L., Raeymaekers, L., Wuytack, F., and Missiaen, L. (2007). Diseases involving the Golgi calcium pump. Subcell Biochem. *45*, 385–404.

Wang, Y., Satoh, A., and Warren, G. (2005). Mapping the functional domains of the Golgi stacking factor GRASP65. J. Biol. Chem. *280*, 4921–4928.

Wang, Y., and Seemann, J. (2011). Golgi biogenesis. Cold Spring Harb. Perspect. Biol. *3*, a005330.

Wang, Y., Seemann, J., Pypaert, M., Shorter, J., and Warren, G. (2003). A direct role for GRASP65 as a mitotically regulated Golgi stacking factor. EMBO J. *22*, 3279–3290.

Wang, Y., Wei, J.H., Bisel, B., Tang, D., and Seemann, J. (2008). Golgi cisternal unstacking stimulates COPI vesicle budding and protein transport. PLoS One *3*, e1647.

Xiang, Y., and Wang, Y. (2010). GRASP55 and GRASP65 play complementary and essential roles in Golgi cisternal stacking. J.Cell Biol. *188*, 237–251.

Xiang, Y., Zhang, X., Nix, D.B., Katoh, T., Aoki, K., Tiemeyer, M., and Wang, Y. (2013). Regulation of protein glycosylation and sorting by the Golgi matrix proteins GRASP55/65. Nat. Commun. *4*, 1659.

Xie, G., Wang, F., Peng, X., Liang, Y., Yang, H., and Li, L. (2018). Modulation of mast cell toll-like receptor 3 expression and cytokines release by histamine. Cell Physiol. Biochem. *46*, 2401–2411.

Xu, C., Ma, H., Inesi, G., Al-Shawi, M.K., and Toyoshima, C. (2004). Specific structural requirements for the inhibitory effect of thapsigargin on the Ca2+ ATPase SERCA. J. Biol. Chem. *279*, 17973–17979.

Zhang, X., Wang, L., Ireland, S.C., Ahat, E., Li, J., Bekier Ii, M.E., Zhang, Z., and Wang, Y. (2019). GORASP2/GRASP55 collaborates with the PtdIns3K UVRAG complex to facilitate autophagosome-lysosome fusion. Autophagy *15*, 1–14.

Zhang, X., Wang, L., Lak, B., Li, J., Jokitalo, E., and Wang, Y. (2018). GRASP55 senses glucose deprivation through O-GlcNAcylation to promote autophagosome-lysosome fusion. Dev.Cell *45*, 245–261.e6.

Zhang, X., and Wang, Y. (2015). GRASPs in Golgi structure and function. Front. Cell Dev. Biol. *3*, 84.

iScience, Volume *23*

Supplemental Information

Cytosolic Ca^{2+} Modulates Golgi Structure Through PKCα-Mediated GRASP55 Phosphorylation

Stephen Ireland, Saiprasad Ramnarayanan, Mingzhou Fu, Xiaoyan Zhang, Jianchao Zhang, Jie Li, Dabel Emebo, and Yanzhuang Wang

Cytosolic Ca^{2+} modulates Golgi structure through PKCα-mediated GRASP55 phosphorylation

Stephen C. Ireland[1], Saiprasad Ramnarayanan[1], Mingzhou Fu[1], Xiaoyan Zhang[1], Jianchao Zhang[1], Jie Li[1], Dabel Emebo[1], Yanzhuang Wang[1,2,*]

[1]Department of Molecular, Cellular and Developmental Biology, University of Michigan, Biological Sciences Building, 1105 North University Avenue, Ann Arbor, MI 48109-1085, USA.
[2]Department of Neurology, University of Michigan School of Medicine, Ann Arbor, MI, 48109-1085, USA.

[*]Correspondence to Yanzhuang Wang (yzwang@umich.edu)

Supplemental Figures and Legends

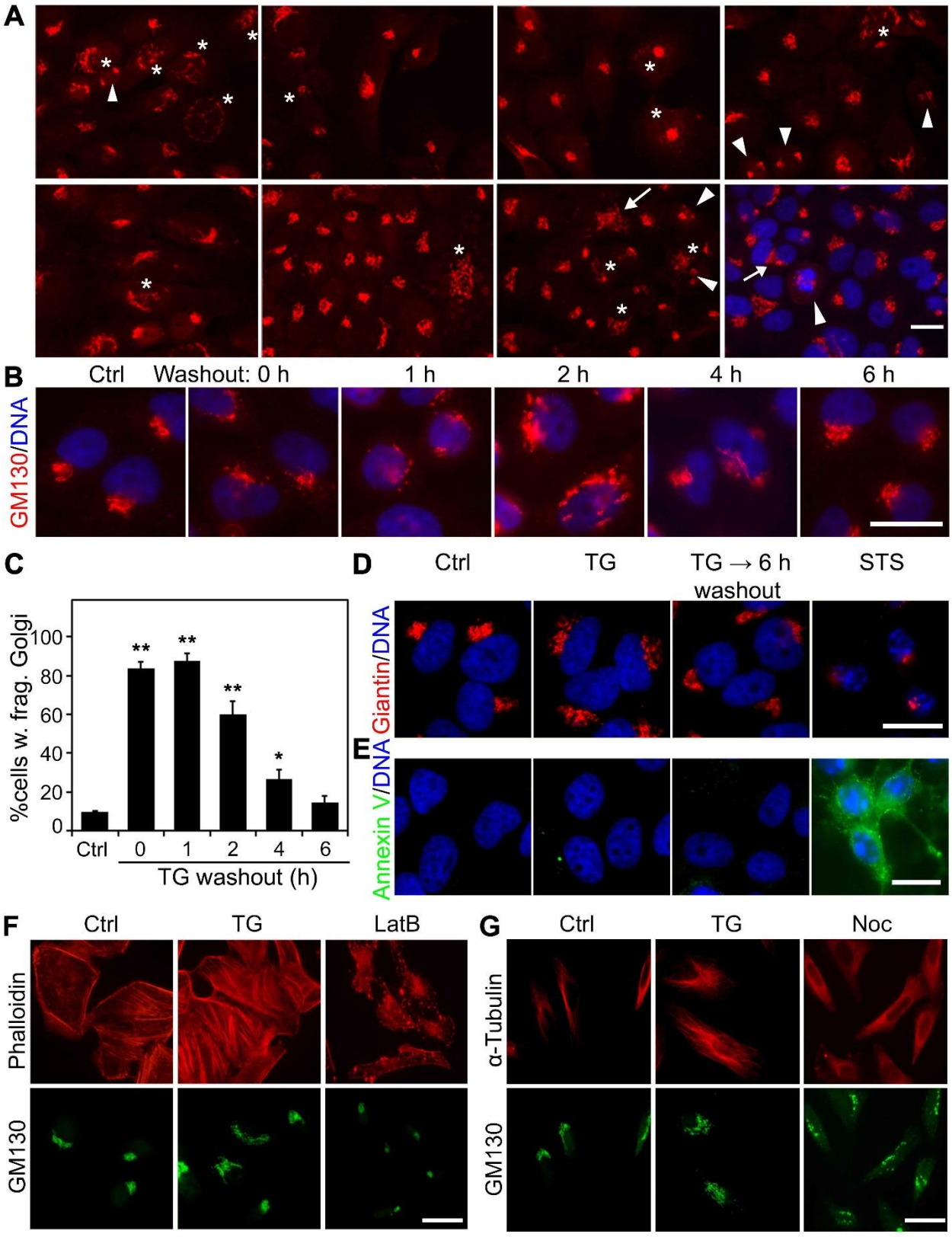

Figure S1. Related to Figure 1. TG-induced Golgi fragmentation is reversible

(A) A gallery of cells with intact or fragmented Golgi. Random images of HeLa cells treated with or without TG were labeled with a GM130 antibody. Asterisks (*) indicate fragmented Golgi, arrowheads

(►) are mitotic Golgi, arrows (→**)** are overlapping Golgi from two or more distinct cells. The last frame includes the DNA channel in blue to show a mitotic cell. **(B)** TG-induced Golgi fragmentation is reversible. Cells were treated with either DMSO or 100 nM TG for 1 h. After washing out TG, TG-treated cells were incubated in fresh growth medium for the indicated times and stained for GM130 and DNA. **(C)** Quantitation of (B) for cells with fragmented Golgi. For statistical analyses, treated cells were compared to the DMSO control (Ctrl). *, $p \leq 0.05$; **, $p \leq 0.01$. **(D)** Acute TG treatment does not cause apoptosis. Cells were treated with either DMSO or 100 nM TG for 20 min without or with 6 h washout, or with 2 μM staurosporine (STS) for 4 h, and stained for GM130 and DNA. **(E)** Cells in (D) were surface stained with Annexin V-EGFP. Scale bars in all fluorescent images, 20 μm. **(F)** Cells were treated with 0.5 μM latrunculin B for 2 h and 250 nM TG was added for the last 20 min. Cells were stained for F-actin with phalloidin (red) and GM130 (green). Scale bar, 20 μm. **(G)** Cells were treated with 1 μM Noc for 2 h and 250 nM TG was added for the last 20 min. Cells were stained for α-tubulin (red) and GM130 (green). Scale bar, 20 μm.

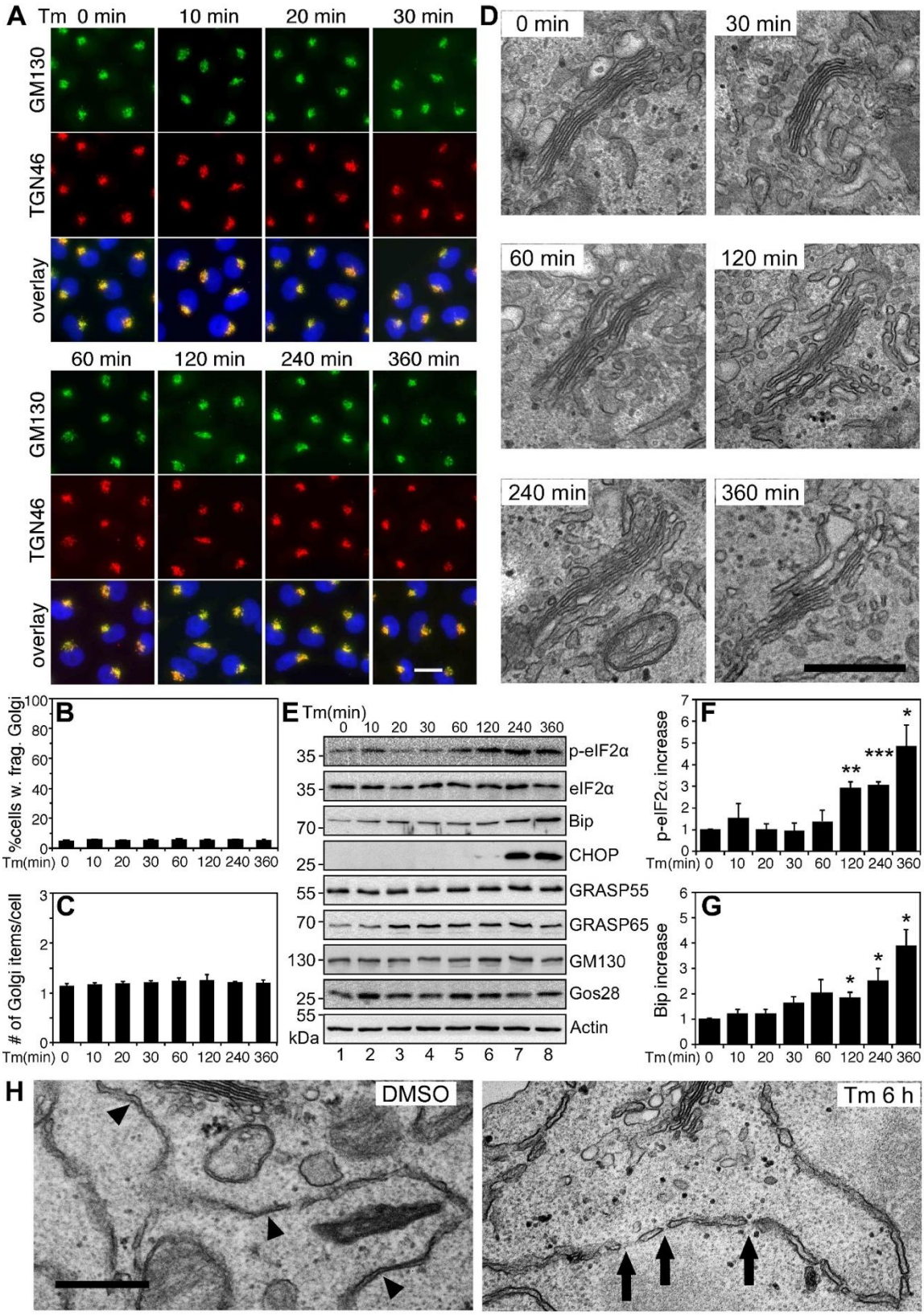

Figure S2. Related to Figure 1. Tm treatment induces UPR but not Golgi fragmentation

(A) Tm treatment has no effect on the Golgi morphology. HeLa cells were treated with 5 μg/ml Tm for indicated times and stained for GM130 and TGN46. Scale bar, 20 μm. **(B-C)** Quantitation of Golgi

fragmentation in Tm-treated cells in (A). **(D)** EM micrographs of the Golgi region in Tm-treated cells. Scale bar, 0.5 µm. **(E)** Tm-treated cells as in (A) were analyzed by Western blots. Note the increased levels of p-eIF2α, Bip and CHOP over time. **(F-G)** Quantitation of p-eIF2α/eIF2α and Bip in (E). Results are shown as Mean ± SEM from at least 3 independent experiments; statistical analyses were performed using two-tailed Student's *t*-tests (*, $p \leq 0.05$; **, $p \leq 0.01$; ***, $p \leq 0.001$). **(H)** Representative EM images of ER cisternae in cells treated with DMSO (Ctrl) or tunicamycin (Tm, 5 µg/ml) for 6 h. ER cisternae in Ctrl cells, indicated by arrowheads (►), appear to have a narrow, intact structure; where in Tm treated cells, the ER cisternae appear to be swollen and fragmented, as indicated by arrows (→). Scale bar, 0.5 µm.

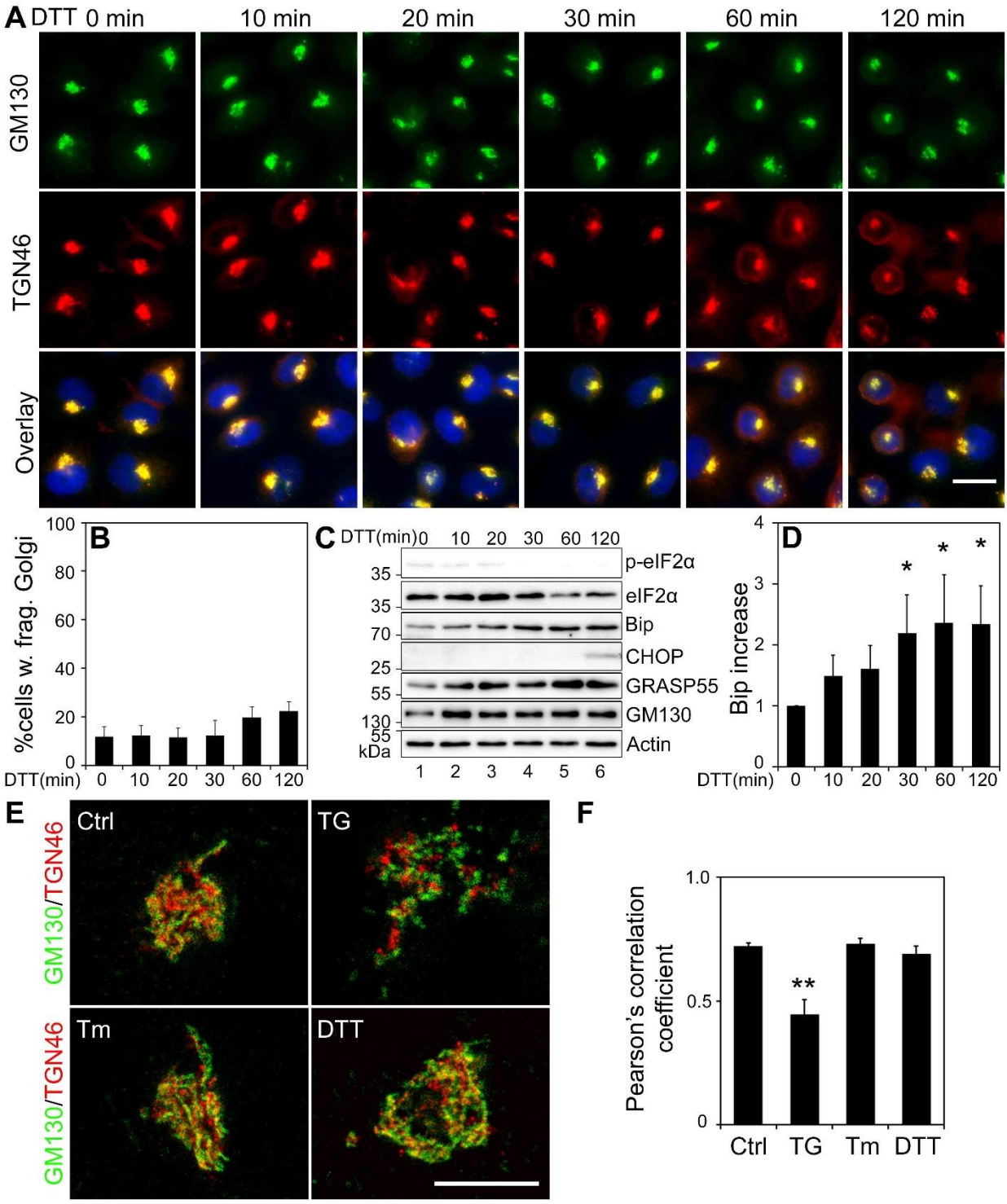

Figure S3. Related to Figure 1. DTT-treatment induces UPR but not Golgi fragmentation

(A) HeLa cells were treated with DMSO or 10 mM DTT for indicated times and stained for GM130 (green), and TGN46 (red). Scale bar, 20 µm. **(B)** Quantitation of (A) for cells with fragmented Golgi. **(C)** Western blots of ER stress and Golgi proteins showing UPR induction upon DTT treatment. **(D)** Quantitation of Bip levels from four independent experiments. Two-tailed Student's *t*-tests were used

to calculate statistical significance (*, $p \leq 0.05$). **(E)** HeLa cells were treated with DMSO, 250 nM TG for 20 min, 5 µM Tm for 6 h, or 10 mM DTT for 2 h. Cells were stained for GM130 (green) and TGN46 (red) and analyzed by super-resolution microscopy. **(F)** Pearson's correlation coefficients of GM130 and TGN46 signals in (E). Two-tailed Student's *t*-tests were used to calculate statistical significance (**, $p \leq 0.01$).

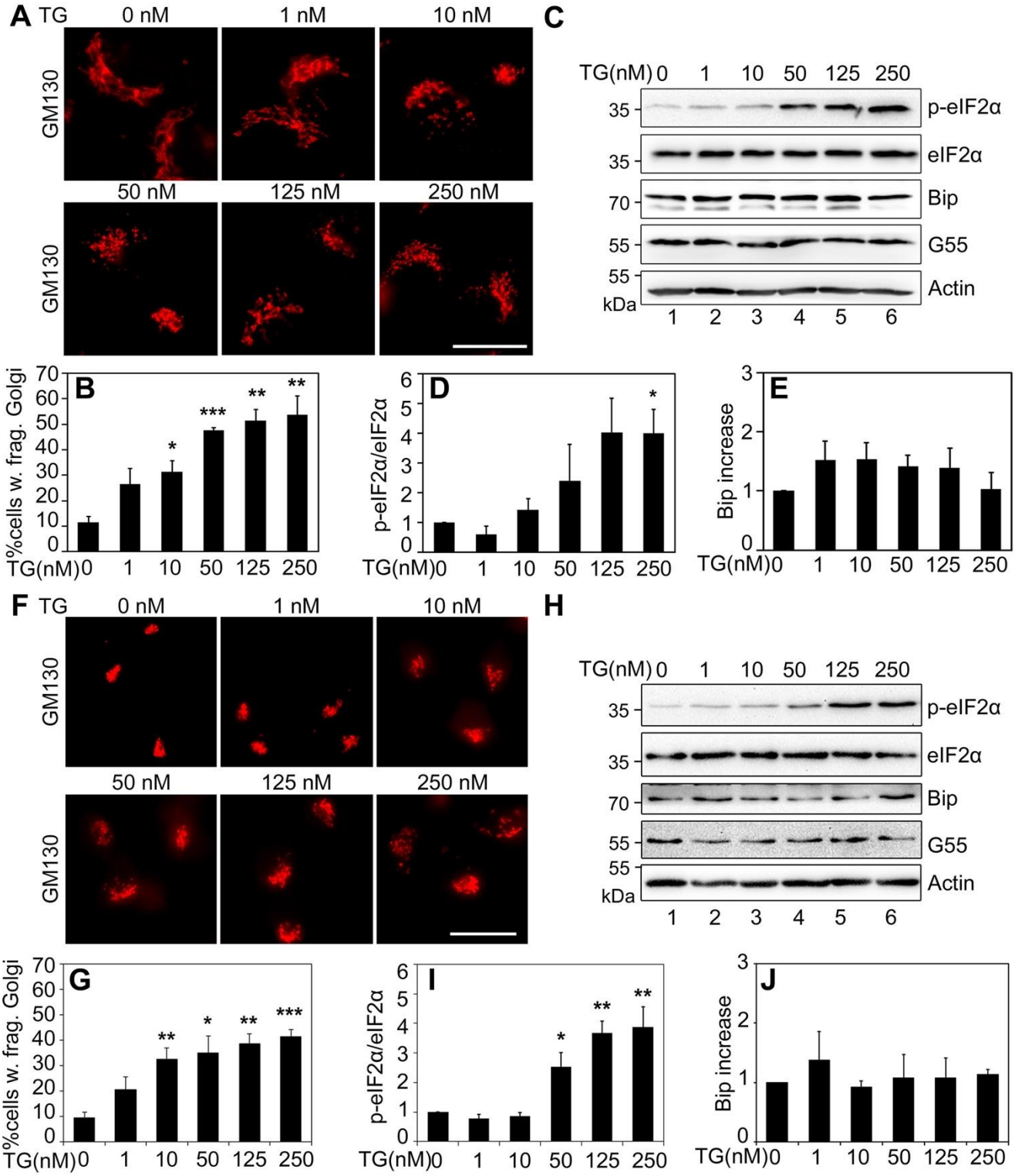

Figure S4. Related to Figure 2. Low concentration of TG induces Golgi fragmentation in NRK cells and RAW 264.7 macrophages

(A) NRK cells were treated with the indicated concentrations of TG for 20 min and stained for GM130. Scale bar, 20 μm. **(B)** Quantitation of cells with fragmented Golgi in (A). **(C)** Cells treated

with TG as in (A) were analyzed by Western blots. **(D-E)** Quantitation of p-eIF2α/eIF2α and Bip in (C) from 3 independent experiments. **(F)** RAW 264.7 murine macrophage cells were treated with the indicated concentrations of TG for 20 min and stained for GM130. Scale bar, 10 μm. **(G)** Quantitation of cells with fragmented Golgi in (F). **(H)** Cells treated with TG as in (F) were analyzed by Western blots. **(I-J)** Quantitation of p-eIF2α/eIF2α and Bip in (H) from 3 independent experiments. Two-tailed Student's *t*-tests were used to calculate statistical significance (*, $p \leq 0.05$; **, $p \leq 0.01$; ***, $p \leq 0.001$).

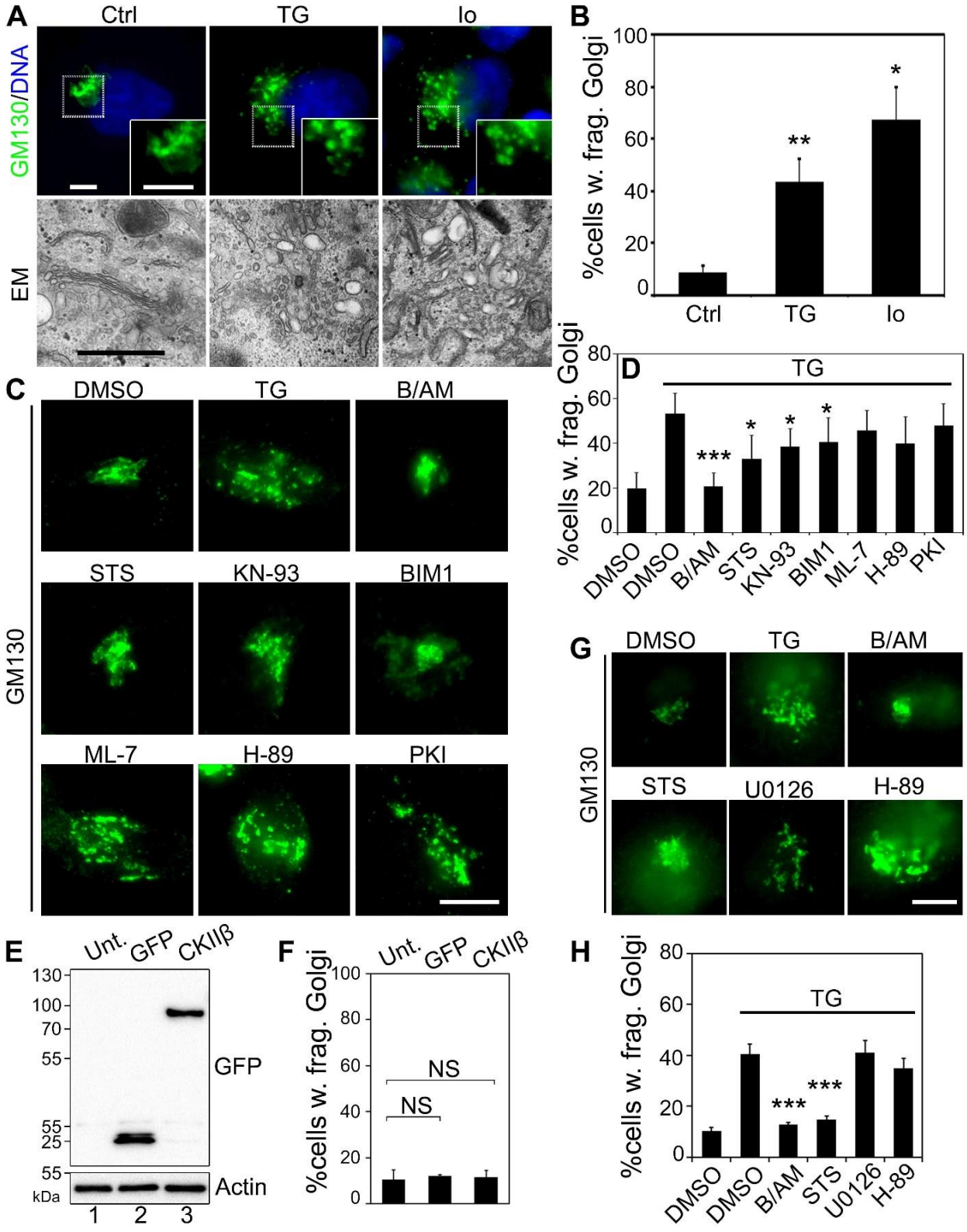

Figure S5. Related to Figure 2-3. Identification of PKC as the kinase for TG-induced Golgi fragmentation

(A) HeLa cells were treated with DMSO (Ctrl), 100 nM TG, or 1 μM ionomycin (Io) for 1 h, and analyzed by fluorescence microscopy (top panels) and EM (lower panels). Boxed regions are enlarged

in the insets. Scale bars on the fluorescence images, 5 µm; scale bar on EM micrographs, 0.5 µm. **(B)** Quantitation of cells with fragmented Golgi in (A) based on the GM130 pattern. **(C)** PKC inhibition reduces TG-induced Golgi fragmentation. Cells were pre-treated with 60 µM BAPTA-AM (B/AM), 2 µM staurosporine (STS), 5 µM KN-93, 2 µM BIM1, 5 µM ML-7, 30 µM H-89, or 10 µM PKI for 10 min, followed by the treatment with either DMSO or 250 nM TG for 20 min, and stained for GM130. Scale bar, 10 µm. **(D)** Quantitation of (C) for Golgi fragmentation. Experiments were quantified in a double-blinded fashion and results from three independent experiments were used to calculate means ± SEM. **(E)** Western blot of cells transfected with GFP or GFP-CAMKIIβ using a GFP antibody. **(F)** Quantitation of cells with fragmented Golgi in cells transfected with GFP or GFP-CAMKIIβ as in (E). For statistics, transfected cells were compared to control untransfected (Unt.) cells. **(G)** HeLa cells were treated with MAPK/ERK or PKA/PKD inhibitors, U0126 and H-89, respectively, followed by 100 nM TG treatment for 20 min. **(H)** Quantitation of Golgi fragmentation in (G). Two-tailed Student's *t*-tests were used to calculate statistical significance (*, $p \leq 0.05$; **, $p \leq 0.01$; ***, $p \leq 0.001$).

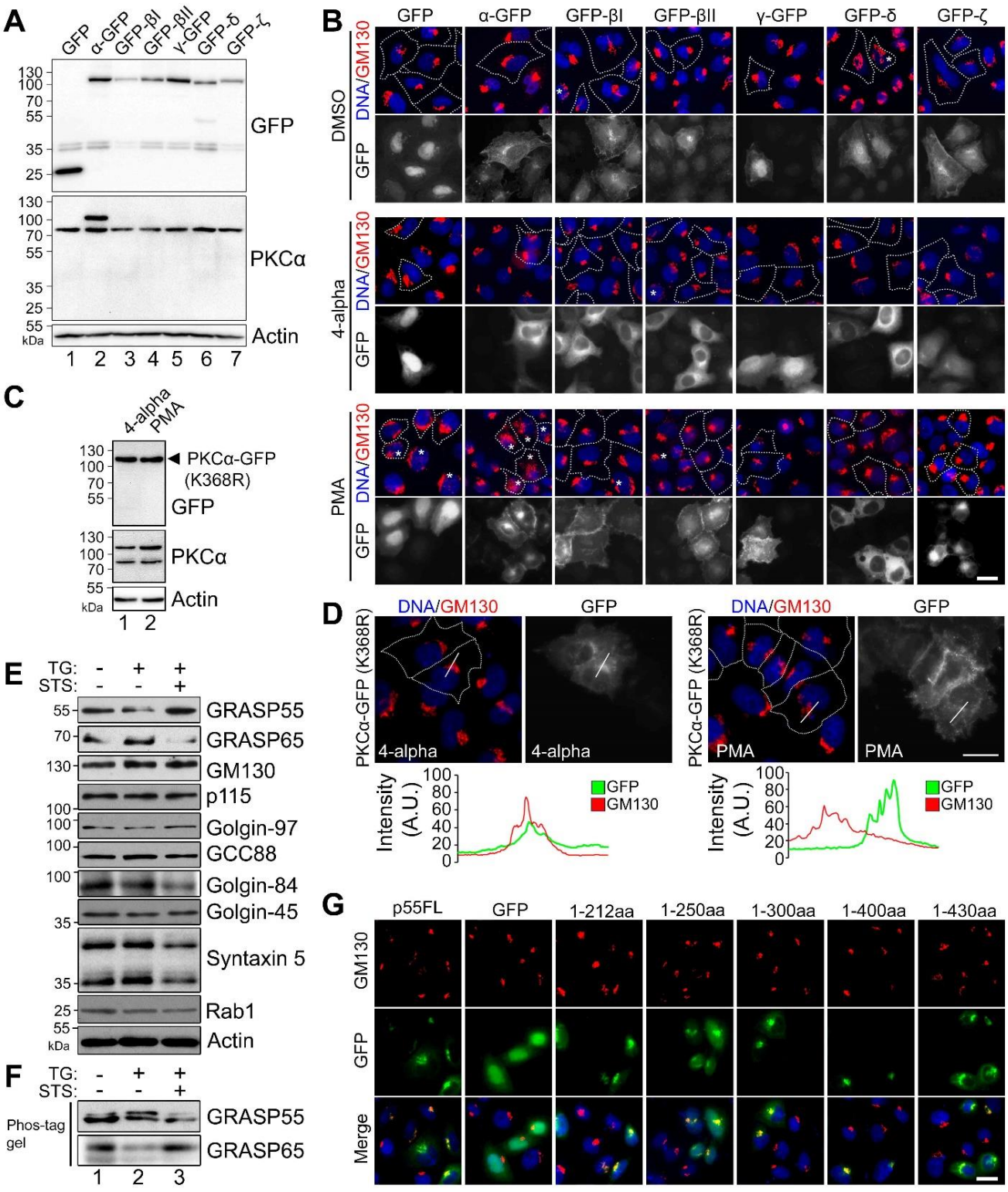

Figure S6. Related to Figure 4-5. PKCα localizes to the Golgi upon activation

(A) Expression of PKC isoforms. HeLa cells were transfected with indicated PKC isoforms and analyzed by Western blot for GFP or PKCα. **(B)** Fluorescent images showing the localization of expressed PKC isoforms after treatment with DMSO, 4-alpha, or PMA. PMA induces PKCα (α-GFP)

localization to the Golgi area, a similar but less dramatic effect was observed for PKCβII (GFP-βII). Scale bar, 20 μm. **(C)** PKCα-GFP (K368R) expressed in HeLa cells and treated with either 4-alpha or PMA and visualized by Western blotting. **(D)** Cells in (C) were probed for GM130 (red) and DNA (blue). To quantify the localization of PKC relative to the Golgi in these images, relative fluorescence intensity was plotted along a random line through the Golgi region. Note the agreement in peaks in control (left side) and relative disagreement in peaks in the PMA stimulated cell (right side). Scale bar, 20 μm. **(E)** TG treatment results in the phosphorylation of GRASP55 but not other Golgi proteins. HeLa cells were treated with 250 nM TG for 1 h, with or without 2 μM staurosporine (STS) pre-treatment for 10 min, and analyzed by Western blot. **(F)** Cell lysates in (E) were analyzed by phos-tag gels and Western blot. **(G)** Immunofluorescence images of cells expressing indicated GRASP55 truncation mutants.

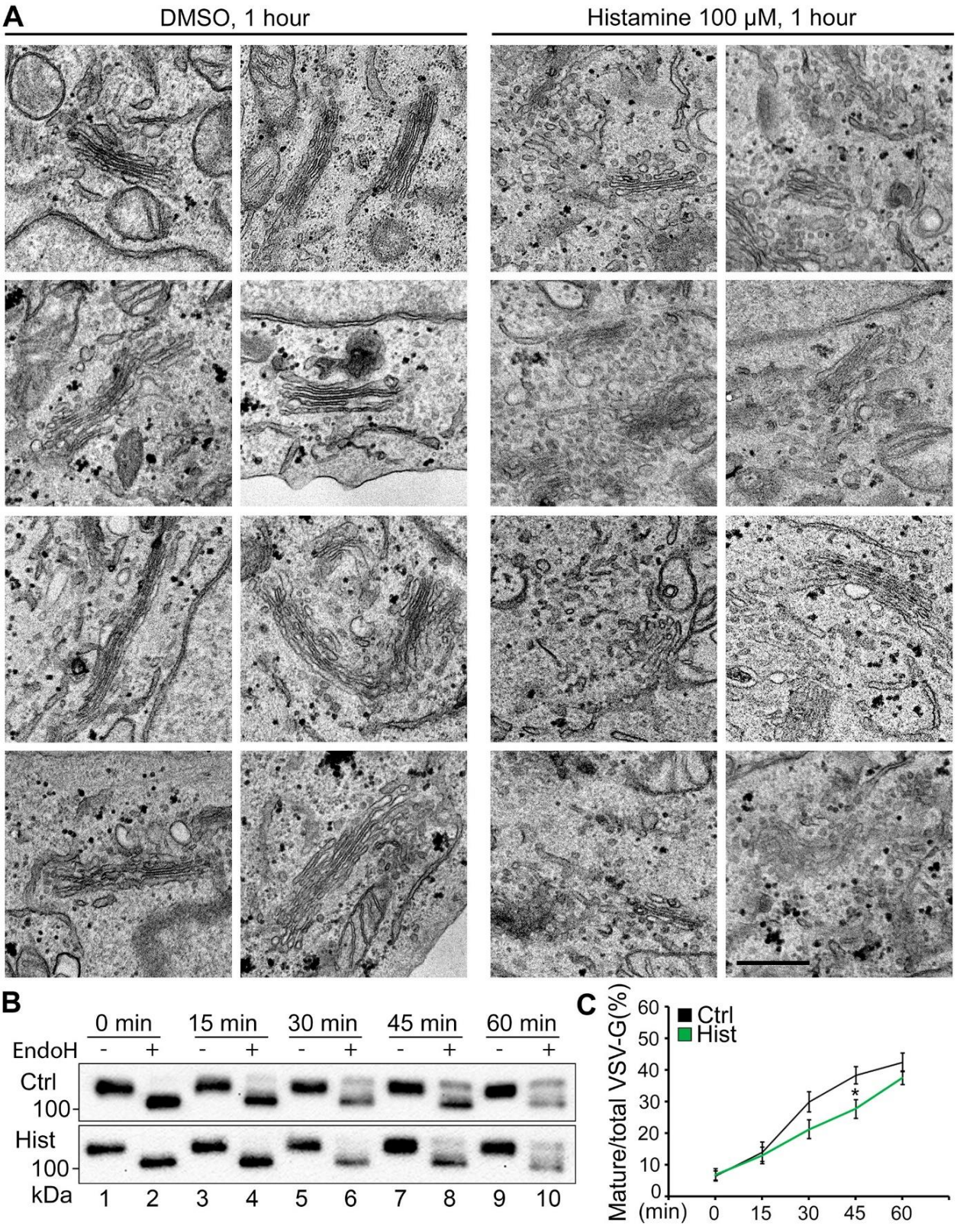

Figure S7. Related to Figure 6. Histamine treatment alters the Golgi structure

(A) HeLa cells treated with either DMSO (control, 1 h) or histamine (100 µM, 1 h) were analyzed by EM. Shown are collections of electron micrographs representing the two treatments. Consistent

aberrations in Golgi shape were frequently seen in histamine-treated cells, including reduced cisternae number and stack length, and increased number of vesicles. Scale bar, 0.5 µm. **(B)** Cells were transfected with the Str-li_VSVG wt-SBP-EGFP plasmid for 16 h and treated without (Ctrl) or with 100 µM histamine (Hist) at 37°C for 1 h. Cells were then incubated with complete medium containing 40 µM biotin and 100 µM of Hist, lysed at the indicated time points, and treated without (-) or with (+) EndoH, and analyzed by Western blot. **(C)** Quantification of (B) for the percentage of EndoH resistant VSV-G from 3 independent experiments. All quantitation results are shown as Mean ± SEM. Statistical analyses were performed using two-tailed Student's *t*-tests (*, $p \leq 0.05$).

TRANSPARENT METHODS

Reagents, Plasmids and siRNA

All reagents used were from Sigma-Aldrich (St. Louis, MO), Roche (Basel, Switzerland) or Calbiochem (EMD Millipore, Burlington, MA), unless otherwise stated. The Annexin V apoptosis detection kit was from BioVision Inc. (San Francisco, CA). PKCα-GFP and GFP-PKCβII plasmids were provided by Dr. Yusuf Hannun (Stony Brook Cancer Center). GFP-PKCβI, GFP-PKCδ, and GFP-PKCζ plasmids were provided by Dr. Hesham El-Shewy (Medical University of South Carolina). The CAMKIIβ plasmid was provided by Dr. Mohammed Akaaboune (University of Michigan). The Str-li_VSVGwt-SBP-EGFP plasmid was provided by Dr. Franck Perez (Institut Curie). PKCγ-GFP cDNA construct was purchased from Addgene (Cambridge, MA). The ManII-GFP HeLa cell line was made in house by transfecting HeLa cells with α-mannosidase II covalently linked to GFP. Control siRNA (Silencer Select Negative Control #1 siRNA) was purchased from Applied Biosystems (ThermoFisher). PKC-specific custom siRNA targeting to endogenous human PKCα (5'-CAGAAGAACTGTATGCAAT-3') was purchased from Ambien (ThermoFisher). To perform knockdowns, 200 nM of each oligo was used to transfect cells for 48 hours.

Antibodies

The following antibodies were used: monoclonal antibodies against β-actin and GFP (Sigma-Aldrich), Gos28 and GM130 (BD Biosciences, Franklin Lanes, NJ), PKCα (Santa Cruz Biotechnology, Dallas, TX), and α-tubulin (Developmental Studies Hybridoma Bank, University of Iowa); polyclonal antibodies against CHOP, p-eIF2α, eIF2α and p115 (Cell Signaling, Danvers, MA), Giantin, GRASP55 and GRASP65 (Proteintech), Bip (Santa Cruz), GM130 ("N73" from Dr. J. Seemann), and TGN46 (Bio-Rad). Secondary antibodies were purchased from Jackson Laboratory (Bar Harbor, ME). Secondary antibodies used for fluorescence microscopy include fluorescence-labelled goat anti-mouse, goat anti-rabbit and goat anti-sheep (for TGN46) antibodies, all used in 1:200 dilution. Secondary antibodies used for Western blot include HRP-conjugated goat anti-mouse and goat anti-rabbit antibodies, all used in 1:5000 dilution.

Molecular Cloning

Constructs for GRASP55 truncation mutants, aa1-212, aa1-250, aa1-300, aa1-400, aa1-430 were constructed in pEGFP-N1 vector using BamHI and HindIII sites (Zhang et al., 2018). Catalytically

inactive PKCα, PKCα-GFP (K368R), was made in-house using site-directed mutagenesis. The genetically encoded calcium indicator GRASP55-GCaMP7 was made in-house by inserting the GCaMP7a gene (kind gift from Dr. Haoxing Xu) into a pmCherry-N1-GRASP55 WT vector (Zhang et al., 2018) using BamH1 and NotI restriction sites. All cDNAs generated in this study were confirmed by DNA sequencing.

Cell Culture and Drug Treatments

For all experiments, mycoplasma-free HeLa were obtained from ATCC (Manassas, VA) and passaged ≤20 times prior to use in experiments. NRK cells were a gift from Dr. Peter Arvan (University of Michigan). HeLa and NRK cells were cultured in Dulbecco's modified Eagle's medium (DMEM; ThermoFisher, Waltham, MA) supplemented with 10% fetal bovine serum (FBS; Gemini Bio-Products, Sacramento, CA) and 100 units/ml penicillin-streptomycin at 37°C with 5% CO_2. RAW 264.7 murine macrophages were kindly provided by Dr. Kezhong Zhang (Wayne State University) and cultured in RPMI 1640 medium supplemented with 10% fetal bovine serum and 100 units/ml penicillin-streptomycin at 37°C with 5% CO_2. Cells were grown on glass coverslips according to standard tissue culture methods (Tang et al., 2012). Coverslips were pre-coated with poly-lysine (Gibco) to aid in cell attachment. For mitotic synchronization, cells were treated with 100 ng/ml nocodazole for 18 h and "shake-off" cells (Xiang et al., 2007) were collected and lysed for Western blot analysis. All drugs, except cAMP-dependent protein kinase inhibitor (PKI) that is a peptide and dissolved in water, were made in DMSO, aliquoted, and stored at -20ºC. Stocks were diluted into working solutions of DMEM at the time of the experiment as described in the text or figure legend. Upon the addition of the drug, cells were incubated at 5% CO_2 and 37°C for the indicated times. Cells were washed 3 times with ice cold phosphate buffered saline (PBS) and collected with a cell scraper.

Immunofluorescence Microscopy

For fluorescence microscopy, cells were rinsed 3 times in ice cold PBS, fixed with 4% (w/v) paraformaldehyde, quenched with 50 mM NH_4Cl, permeabilized in 0.2% v/v Triton X-100 in PBS, and blocked for 1 h with PBS with 1% w/v bovine serum albumin (BSA) Fraction V (ThermoFisher, Waltham, MA) (Tang et al., 2016). Cells were incubated with a primary antibody diluted in 1% BSA in PBS (PBSB) at room temperature for 1.5 h, washed with PBS, and incubated with an FITC- or TRITC-labeled secondary antibody (1:200 dilution) in PBSB for 45 min at room temperature. Cells were washed 3 times with PBS and stained with 1:5,000 Hoechst dye for 5 min, mounted on glass slides with Moviol, and images were captured with a Zeiss (Oberkochen, Germany) Observer

fluorescent microscope with a 63x oil objective lens with a numerical aperture of 1.4 and an Axiocam Mrm camera. TIF files were exported with AxioVision software (Zeiss).

For super-resolution microscopy, Alexa Fluor 647, and Alexa Fluor 488-labeled secondary antibodies (ThermoFisher) were used. After washing, coverslips were mounted to slides using ProLong Diamond antifade super-resolution imaging mountant (ThermoFisher). Super-resolution images were imaged using Leica (Wetzlar, Germany) TCS SP8 STED super-resolution microscope. Images were quantified using the NIH ImageJ software and assembled into figures with Photoshop Elements (Adobe, San Jose, CA). To clearly show the Golgi structure, brightness or contrast was adjusted linearly across all samples within each experiment.

For calcium imaging, GRASP55-GCaMP7 transfected cells were plated onto glass bottomed dishes and imaged by a Nikon C2-plus Laser Scanning Confocal Microscope System configured with a Ti2-E inverted microscope. Images were captured at 488 nm and 561 nm in sequential scanning mode. Z-stacks of 5 slices at 1 μm interval were acquired every 30 seconds for a total period of 10 min. The NIS-Elements C software was used for acquisition, analysis and visualization. The "+Histamine" symbol in Movie S1 was added in Adobe Premiere Pro 2020. For quantification, fluorescence intensity was measured every minute for 60 min. 20 cells were measured for each drug treatment.

To quantify Golgi fragmentation, cells were evaluated by eye under a microscope according to predefined fragmentation criteria, at least 300 cells were counted in each reaction. The following criteria are used to define whether a Golgi is intact or fragmented: 1) If the Golgi exists as a single piece of connected membrane, it is intact. 2) If a Golgi exhibits several items that are connected by visible membrane bridges, even though these bridges might be faint, the Golgi is considered intact. 3) If a Golgi exhibits ≥ 3 disconnected pieces (no visible bridges connecting them), then the Golgi is fragmented. 4) Mitotic cells, defined by the DNA pattern, and overlapping cells in which the Golgi pattern is difficult to define, are not counted. Hoechst was used to identify individual, mitotic and overlapping cells. In experiments where transfected proteins were employed, only transfected cells were counted, and 100 cells were counted per replicate. In experiments where an inhibitor screen was performed, an unbiased image thresholding method was used to extract fragmentation data from ≥40 cells per replicate.

Electron Microscopy (EM)

For EM, cells were fixed in pre-warmed serum-free DMEM, 20 mM Hepes, pH 7.4, 2% glutaraldehyde at room temperature for 30 min or 4°C overnight as previously described (Tang et al., 2010). Cells were washed 2 times with 0.1 M Sodium cacodylate (Electron Microscopy Sciences, Hatfield, PA), and post-fixed on ice in 1% v/v reduced Osmium tetroxide, 0.1 M Sodium cacodylate (w/v) and 1.5% cyanoferrate (w/v) in water. Cells were rinsed 3 times with 50 mM maleate buffer, pH 5.2, 3 times with water, scraped, and pelleted in microcentrifuge tubes for embedding. The EMBED 812 (EMD) protocol was used to embed cells and resin blocks were sectioned to 60 nm with a diamond knife and mounted on Formvar-coated copper grids. Samples were double contrasted with 2% uranyl acetate then with lead citrate and rinsed with copious amounts of water. Grids were imaged using a Philips (Amsterdam, Netherlands) transmission electron microscope. Golgi images were captured at 11,000x magnification. Golgi stacks were identified using morphological criteria and quantified using standard stereological techniques. A Golgi cisterna was identified as a perinuclear membrane within a Golgi stack ≥4 times longer than its width. Stack length was measured for the longest cisterna within a Golgi stack using the ruler tool in Photoshop Elements 13. For the number of cisternae per stack, the number of cisternae was counted. For the number of vesicles per stack, round objects no greater than 80 µm in diameter within 0.5 µm of a Golgi stack were counted. At least 20 cells were quantified in each experiment, and the EM results represent two independent experiments.

Protein Biochemistry

For immunoblotting, cells from a culture dish were pelleted and lysed with 30 µl lysis buffer (40 mM Hepes, pH 7.4, 200 mM KCl, 5 mM $MgCl_2$, 1% Triton X-100 (Bio-Rad, Hercules, CA), 50 mM beta-glycerol phosphate, protease inhibitor cocktail (Roche), and phosphatase inhibitors NaF and NaVan pH 8.0). Samples were mixed with 6X SDS-PAGE sample buffer (400 mM Tris-Cl pH 6.8, 15% SDS, 10 mM DTT, 50% glycerol, 0.05% bromophenol blue), denatured at 95°C for 4 min and then run on PAGE gels. For figures 5, subpanels A, C and D, 8% phos-tag gels were run at 4°C for 8 h. Protein was transferred to nitrocellulose membranes using semi-dry transfer (Bio-Rad, Hercules, CA) at constant 16 V. Membranes were blocked for 10 min with 3% milk in 0.2% Tween-20 in phosphate buffered saline (PBST) and immunoblotted. Western blots were captured with Enhanced Chemiluminescence (ECL) dye reagent (ThermoFisher), in a FluorChem M chemi-luminescent imager (ProteinSimple, San Jose, CA).

VSV-G Trafficking using RUSH system

VSV-G trafficking was performed as previously described (Li et al., 2019). Briefly, HeLa cells were transfected with the Str-li_VSVG wt-SBP-EGFP plasmid (Boncompain et al., 2012) and cultured at 37°C for 16 h. Cells were then incubated with 250 nM TG or 10 µM monensin in fresh medium for 0.5 h at 37°C before 40 µM D-biotin (VWR Life Science, Radnor, PA) was added. Cells were then lysed at indicated time points (chase), treated with or without EndoH, and analyzed by Western blotting for VSV-G-GFP using a GFP antibody. The percentage of EndoH resistant VSV-G was quantified using the ImageJ software.

In vitro Kinase Assay

Twenty µg/ml recombinant GRASP55 protein (Xiang and Wang, 2010) was incubated with 10 µg/ml recombinant PKCα (SignalChem, British Columbia, Canada) in the presence or absence of 2 mM ATP. Reactions were performed in kinase buffer (20 mM HEPES-NaOH, pH 7.4, 1 mM $CaCl_2$, 1 mM DTT, 10 mM $MgCl_2$, 200 µg/ml phosphatidylserine, 20 µg/ml diacylglycerol) at 30°C for 3 h. Reactions were terminated by adding SDS sample buffer and boiling. GRASP55 proteins were separated by Phos-tag SDS-PAGE and visualized by immunoblotting. In brief, 50 µM Phos-tag acrylamide and 100 µM $MnCl_2$ were included in the gel recipe according to the manufacturer's instructions. Phos-tag gels were washed three times in transfer buffer supplemented with 10 mM EDTA and twice in transfer buffer without EDTA before transferring to membranes. Proteins were visualized by Western blotting.

Quantitation and Statistics

All data represent the mean ± SEM (standard error of the mean) of at least three independent experiments unless noted. A statistical analysis was conducted with two-tailed Student's t-test in the Excel program (Microsoft, Redmond, WA). Differences in means were considered statistically significant at $p \leq 0.05$. Significance levels are: *, $p<0.05$; **, $p<0.01$; ***, $p<0.001$. Figures were assembled with Photoshop (Adobe, San Jose, CA). Pearson's colocalization coefficient values were computed using the "Coloc 2" function in ImageJ software.

References

Boncompain, G., Divoux, S., Gareil, N., de Forges, H., Lescure, A., Latreche, L., Mercanti, V., Jollivet, F., Raposo, G., and Perez, F. (2012). Synchronization of secretory protein traffic in populations of cells. Nat Methods *9*, 493-498.

Li, J., Tang, D., Ireland, S.C., and Wang, Y. (2019). DjA1 maintains Golgi integrity via interaction with GRASP65. Molecular biology of the cell *30*, 478-490.

Tang, D., Xiang, Y., and Wang, Y. (2010). Reconstitution of the cell cycle-regulated Golgi disassembly and reassembly in a cell-free system. Nat Protoc *5*, 758-772.

Tang, D., Yuan, H., Vielemeyer, O., Perez, F., and Wang, Y. (2012). Sequential phosphorylation of GRASP65 during mitotic Golgi disassembly. Biology open *1*, 1204-1214.

Tang, D., Zhang, X., Huang, S., Yuan, H., Li, J., and Wang, Y. (2016). Mena-GRASP65 interaction couples actin polymerization to Golgi ribbon linking. Molecular biology of the cell *27*, 137-152.

Xiang, Y., Seemann, J., Bisel, B., Punthambaker, S., and Wang, Y. (2007). Active ADP-ribosylation factor-1 (ARF1) is required for mitotic Golgi fragmentation. J Biol Chem *282*, 21829-21837.

Xiang, Y., and Wang, Y. (2010). GRASP55 and GRASP65 play complementary and essential roles in Golgi cisternal stacking. J Cell Biol *188*, 237-251.

Zhang, X., Wang, L., Lak, B., Li, J., Jokitalo, E., and Wang, Y. (2018). GRASP55 Senses Glucose Deprivation through O-GlcNAcylation to Promote Autophagosome-Lysosome Fusion. Developmental cell *45*, 245-261 e246.